






Cite this: *Biomater. Sci.*, 2022, **10**, 4392

## Antimicrobial mechanisms of biomaterials: from macro to nano

Shounak Roy,  <sup>†a</sup> Sanchita Sarkhel, <sup>†a</sup> Deepali Bisht, <sup>a</sup> Samerender Nagam Hanumantharao, <sup>b</sup> Smitha Rao  <sup>b</sup> and Amit Jaiswal  <sup>\*a</sup>

Overcoming the global concern of antibiotic resistance is one of the biggest challenges faced by scientists today, and the key to tackling this issue of emerging infectious diseases is the development of next-generation antimicrobials. The rapid emergence of multi-drug resistant microbes, superbugs and mutated strains of viruses has fuelled the search for new and alternative antimicrobial agents with broad-spectrum biocidal activity. Biomaterials, ranging from macroscopic polymers, proteins, and peptides to nanoscale materials such as nanoparticles, nanotubes and nanosheets have emerged as effective antimicrobials. An extensive body of research has established the antibacterial and antiviral efficiencies of different types of biomaterials. What make these materials unique are the different modes through which they interact and exert their antimicrobial activity. This review provides a comprehensive and detailed overview of the diverse modes of interaction between biomaterials and bacteria and viruses, and sheds light on how different biomaterials influence and modulate antimicrobial mechanisms to achieve a high degree of therapeutic efficacy without resistance generation.

Received 29th March 2022,  
Accepted 3rd June 2022  
DOI: 10.1039/d2bm00472k  
rsc.li/biomaterials-science

### 1. Introduction

Recently, the increasing numbers of fatalities related to infectious diseases<sup>1–4</sup> have been higher than those attributable to terrorism, weapons of mass destruction and wars combined. This has led to global concern and a shift in focus towards identification, prevention, and treatment of the diseases,<sup>5,6</sup> particularly

<sup>a</sup>School of Basic Sciences, Indian Institute of Technology Mandi, Kamand, Mandi, Himachal Pradesh, Pincode: 175075, India. E-mail: j.amit@iitmandi.ac.in

<sup>b</sup>Department of Biomedical Engineering, Michigan Technological University, Houghton, MI 49931, USA

<sup>†</sup>Equal contributing authors.



Shounak Roy

Shounak Roy received a Master of Science degree in genetic engineering from the West Bengal University of Technology, India, in 2013. Following this, he received a Master of Technology degree in Biotechnology from the Birla Institute of Technology Mesra, Ranchi, India, in 2015. He received the INSPIRE fellowship from the Department of Science and Technology, Government of India in 2017 to pursue a Ph.D. Currently, he is a

Ph.D. candidate at the Indian Institute of Technology, Mandi in the School of Basic Sciences under the supervision of Dr Amit Jaiswal. His main research interests include the synthesis of novel 2D material-based nanocomposites for the development of cancer therapeutics and nano-antimicrobials.



Sanchita Sarkhel

Sanchita Sarkhel did her Bachelor's degree in Microbiology at the University of Calcutta. After that, she completed her Master's degree in Microbiology from St. Xavier's College, Kolkata. Currently, she is pursuing her Ph.D. at the Indian Institute of Technology, Mandi, under the guidance of Dr Amit Jaiswal. Her primary research interest lies in biomaterials with antimicrobial and wound healing properties.

air-borne respiratory diseases, antibiotic-resistant bacterial infections (ARBI) and what are known as super bugs.<sup>7</sup> Traditional therapies used against the ARBI have combined different antibiotics, while vaccinations are used to prevent viral infections.<sup>8–10</sup> However, the effectiveness of a combination of antibiotics differs, with possible side effects, and hence cannot be optimized. Currently available antiviral targets are very specific to the virus and have differential results based on clinical experience.<sup>11</sup> Thus, the widespread emergence of ARBI and novel strains of virus such as SARS-CoV-2 has demonstrated the need for novel techniques for prevention, diagnosis, and therapies.

Biomaterials, from macromolecules such as polymers and proteins to nanoparticles belonging to different dimensions, have emerged as promising antimicrobial alternatives to the existing therapeutics. Even before the emergence of antibiotics, antimicrobial peptides (AMP) played a big role in host defense against infection. And for the same reason they are also referred to as host defense peptides. AMPs are low molecular weight peptides of 8–100 amino acids, mainly cationic and amphipathic in nature, and show broad-spectrum activity. They are present almost ubiquitously from prokaryotes to eukaryotes.<sup>12</sup> The discovery of antibiotics<sup>13</sup> overshadowed the importance of AMPs to an extent, but the rapid emergence of antibiotic resistance among pathogens has brought back attention to AMPs again as a potential agent for antimicrobial activity. Because of some drawbacks like stability, hemolytic activity *etc.*, naturally occurring AMPs have limited applications. To overcome this problem, various synthetic analogs of AMPs like cationic peptides and peptide mimics, and macromolecules like polymers and peptidopolysaccharides have come into play. Some naturally occurring biomolecules like polysaccharides have intrinsic antibacterial activity, whereas others have been developed through chemical modifications of the natural polymeric backbone.<sup>14</sup> Cationic peptides and synthetic peptide mimics, which basically mimic the backbone of naturally occurring AMPs but have additional functional groups attached to them, also make for very potent antibacterial biomaterials.<sup>15</sup> Furthermore, pepti-

dopolysaccharides, which are combinations of peptides and polysaccharides, possess the ability to mimic the bacterial peptidoglycan layer and show antibacterial activity by interfering with bacterial cell wall synthesis.<sup>16</sup>

Similarly, there have been tremendous developments in the field of nanoscience in the past decade in the development of next-generation antimicrobials. The definition of nanomaterials is different based on the legislating organizations. The general definition classifies materials of the scale of 1–100 nm in at least one dimension and exhibiting properties distinct from their bulk counterpart as nanomaterials. The nanomaterials can have different structures: spheres, rods, wires, ribbons, tubes, scaffolds, fibers, beads or sheets.<sup>17</sup> Further, their origin can be carbon based, inorganic, organic, or composite based. The size-dependent properties and vastly different interactions with their environment promotes the manipulation and use of nanomaterials as anti-microbials.<sup>18</sup>

In addition to bacteria, viruses are another major cause of global health concern.<sup>19</sup> Viruses are protein-coated particles with DNA or RNA as their genetic material and have both living and non-living characteristics. To behave like a living entity, the virus needs to enter its host cell and replicate. Viral replication has six major steps starting from viral adsorption on the host cell surface to new virion release. The traditional antiviral therapies which include antiviral drugs like Acyclovir and Remdesivir<sup>20</sup> specifically target viral enzymes involved in viral DNA or RNA synthesis or inhibit proteases, but the problem with such therapies is that viruses quickly mutate and generate resistance against these agents. To address this difficulty, biomaterials have again emerged as an immensely good alternative. Especially, the polyvalency of peptides or polymers gives them diverse antiviral functionalities, which poses difficulty for viruses to develop resistance against them easily.<sup>21,22</sup> In parallel, nanoscience also has a promising perspective when it comes to antiviral agents. Different shapes, sizes and chemistry of nanoparticles attack different steps of the viral replication and infection machinery, thereby assaulting viruses from multiple fronts.



**Deepali Bisht**

*Deepali Bisht received her Bachelor of Technology degree in Biotechnology from IMS Engineering College, UP, Ghaziabad, India, in 2019. In 2020, she qualified with GATE Biotechnology, a MHRD-funded scholarship in India and is currently pursuing her Master of Technology degree from the Indian Institute of Technology, Mandi, in the School of Basic Sciences. She is working under the supervision of Dr Amit*

*Jaiswal for her Master's thesis, and her research interest includes 2D nanomaterials and their antimicrobial action mechanism.*



**Samerender Nagam Hanumantharao**

*Dr Hanumantharao is currently a Research Scientist at Neurocarrus Inc., Lincoln, Nebraska, USA. He received his M.S. and Ph.D. in Biomedical Engineering from Michigan Technological University under the supervision of Dr Smitha Rao. He finished his postdoctoral training in the Biomedical Microdevices Lab at Michigan Technological University. His research interests include the*

*synthesis of nanomaterials, drug delivery, tissue engineering and cancer biology.*

Several studies have been carried out so far that have established the broad-spectrum antibacterial and antiviral properties of polymers, peptides and nanoscale biomaterials against a wide variety of bacteria and viruses. These studies have provided readers with detailed insights into the nature of interactions of the wide varieties of biomaterials with different classes of bacteria and viruses, both at structural and molecular level, and how such interactions contribute towards the observed antimicrobial activity. However, it is interesting to note that biomaterials, depending on their class, follow different modes of antimicrobial activity. Several mechanisms of action of these biomaterials have been proposed in the past by independent studies, each shedding light on a different aspect of a particular material's interaction with microbes. Direct physical contact-mediated membrane disruption through pore-forming or non-pore-forming pathways, and oxidative stress causing membrane damage and subsequent cellular oxidation of biomolecules have been proposed as mechanisms of antimicrobial activity.<sup>23</sup>

The key focus of this review is to provide comprehensive and up-to-date knowledge about the current understanding on how biomaterials ranging from macroscale to nanoscale exert their antibacterial and antiviral actions, and specifically present the readers with an organized overview of their different modes of action. However, discussions, comparisons and evaluations of antibacterial and antiviral efficiencies of different biomaterials in terms of their therapeutic dosage are beyond the scope of this review.

## 2. Antimicrobial biomaterials

### 2.1 Macroscale biomaterials

**2.1.1 Antimicrobial peptides.** Antimicrobial peptides and proteins are one of the most abundant components of the cellular system and are synthesized as the first line of defense in multicellular organisms. These peptides can also be present in

prokaryotic cells to protect them from the surrounding environment. Antimicrobial peptides are small molecules, consisting of 8–100 amino acid residues. They can have different types of secondary structures and biochemical characteristics, ranging from  $\alpha$ -helix,  $\beta$ -sheets, and  $\beta$ -sheets with disulfide bond, hence leading to tertiary structures. Even cyclic AMPs are also naturally available.<sup>24</sup> But among all these,  $\alpha$ -helical AMPs with overall cationic charge and hydrophobic residues are the most common. Basic amino acids arginine and lysine are more abundant in AMPs, whereas acidic amino acids glutamic acid and aspartic acids are less abundant. Basic and aromatic amino acids are more often observed in small AMPs.<sup>25</sup> The combination of cationic and hydrophobic moieties provides AMPs with broad-spectrum activity as an antimicrobial agent. Prokaryotic cell membranes are abundant in anionic phospholipids, whereas eukaryotic cell membranes are made up of more zwitterionic phospholipids. This basic difference in membrane composition allows AMPs to attach to the bacterial cell membranes through electrostatic interaction, hence making prokaryotic cell membranes a selective target over eukaryotic membranes.

AMPs are internalized through a non-receptor-mediated pathway. Broadly, they can be classified into naturally occurring and chemically synthesized AMPs, but both of them follow more or less the same mechanism of action. The first ever naturally occurring AMP which was reported in humans was lysozyme from nasal mucous. Presently, more than 2500 AMPs have been reported in the Antimicrobial Peptide Database.<sup>12</sup> Magainin II and  $\beta$ -defensins are some of the most common AMPs that are synthesized as host defense peptides when cells undergo microbial infection.<sup>26,27</sup> Beside immune system-stimulated AMPs, constitutively expressed AMPs are also present in cells and they can be secreted from various sites where microbial infection is possible, such as the oral cavity (Defensins and Cathelicidin),<sup>28</sup> gastrointestinal tract ( $\alpha$ -Defensins HD-5 and HD-6),<sup>29</sup> skin, eye, respiratory tract, and reproductive tract. However, commercial use of naturally occurring AMPs is very limited because of their instability,



**Smitha Rao**

*Dr Smitha Rao is an Assistant Professor in the Department of Biomedical Engineering at Michigan Technological University. Dr Rao received her M.S. and Ph.D. in Electrical Engineering from UT Arlington, Texas, USA. Dr Rao is a senior member of IEEE, and her research interests include micro- and nano-devices and structures, wound healing, and cancer growth and migration.*



**Amit Jaiswal**

*Dr Amit Jaiswal is presently an Associate Professor in the School of Basic Sciences at the Indian Institute of Technology, Mandi, India. Dr Jaiswal is also an associate of the Indian Academy of Sciences, Bangalore, India. He completed his Ph.D. in Nanotechnology at the Indian Institute of Technology, Guwahati, India, and post-doctoral research at Washington University in St. Louis, USA, and Technion – Israel Institute of Technology, Haifa, Israel. His research interest is in the synthesis of nanomaterials for sensing, catalysis, drug delivery and diagnostic applications.*



expensive extraction from host cells and haemolytic activity. To overcome these shortcomings, biological and chemical syntheses of AMPs have been attempted. Biological synthesis of AMPs is much more difficult because it is a time-consuming, tedious and expensive purification process with low yield. Hence, chemical synthesis methods like solid phase synthesis, liquid phase peptide synthesis, and  $\alpha$ -amino acid *N*-carboxyanhydrides ring-opening polymerization (NCA-ROP) peptide synthesis are choices of interest. The first amphipathic polypeptide which was synthesized using the NCA process was P(K<sub>12.5</sub>F<sub>12.5</sub>), in which the hydrophilicity was rendered by the cationic lysine residues, whereas the hydrophobicity was provided by *L*-phenylalanine, *L*-alanine and *L*-leucine residues.<sup>30</sup> Another synthetic AMP with better cytocompatibility is peptide-*g*-polymer 6.<sup>31</sup> The less positive charge of this peptide makes it less cytotoxic and less haemolytic towards human cells. A series of poly(4-vinyl-*N*-alkylpyridinium) with different linear alkyl chains ranging from propyl to hexadecyl was developed by Tiller and co-workers, and showed significant bactericidal activity against *Staphylococcus aureus*.<sup>32</sup>

**2.1.2 Polymeric biomaterials.** Polymers as antimicrobial biomaterials are of huge importance because of their biocompatibility, ease of synthesis, widespread availability and negligible chance of resistance induction in microbes. Polymers show their antimicrobial activity either through direct killing (microbicidal) or by inhibiting the growth of microbes. Polymeric biomaterials possess both antibacterial as well as antiviral properties. Polymeric biomaterials can be broadly classified as naturally occurring and synthetic polymers. The antimicrobial properties of polymers depend on various factors like molecular weight, charge density, chelating capacity, and hydrophobic and hydrophilic residues. Even the physical state of the polymer, pH and temperature of the surroundings affect their activity. The majority of the naturally occurring antimicrobial polymers belong to the class of polysaccharides, with chitosan being the most exploited cationic polysaccharide for antibacterial applications. It is a linear hetero polysaccharide copolymer of  $\beta$ -1,4 linked *D*-glucosamine and *N*-acetyl-*D*-glucosamine containing an overall positive charge because of the presence of amine groups. Thus, at low pH, amino groups get protonated and electrostatically interact with the negatively charged bacterial membrane.<sup>33,34</sup> Chemically modified polysaccharides and synthetic polymers having varied degrees of functionalization with diverse chemical groups also belong to the category of polymeric antimicrobial biomaterials. These can be categorized as (1) polymers with different functional groups, (2) polymers that mimic AMP and (3) peptide-polysaccharides, which are combinations of peptides and polysaccharides. A wide variety of polymers bearing positive and negative charges, like biguanide polymers,<sup>35</sup> quaternary ammonium polymers,<sup>36</sup> phosphonium polymers, *N*-halamine polymers,<sup>37</sup> sulfated polymers,<sup>38</sup> sialylated polymers,<sup>39</sup> and phosphonothioate polymers can be prepared by introducing the respective functionalities to the polymer backbone. Polymeric AMP mimics such as poly(phenylene ethynylene)-based conjugated polymers with amino side

groups show excellent antimicrobial properties and also low toxicity because of their amphipathic structural arrangement.<sup>40</sup> One of the major differences between prokaryotic and eukaryotic cells is that prokaryotic cells have cell walls made of peptidoglycan, whereas eukaryotic cells do not have a cell wall. This makes the peptidoglycan layer a very common target for antimicrobial agents. Peptido-polysaccharides are an interesting class of polymers which mimic the peptidoglycan layer and create an osmotic imbalance in the microbial cells, resulting in the lysis of cells (Fig. 1).<sup>41</sup>

## 2.2 Nanoscale biomaterials or nanomaterials

Gleiter *et al.* classified nanostructures based on their crystallinity and microstructural features, introducing grain boundary engineering without factoring in the dimensionality.<sup>42</sup> The classification was further developed by Pokropivny *et al.* by using dimensionality of the nanostructures.<sup>43</sup> Pokropivny and Skorohod's method of classification can be used to classify most nanostructures except a few which demonstrate the properties of more than one class. Based on the number of dimensions that lie outside the nanoscale range, nanomaterials can be classified as 0-D, 1-D, 2-D, and 3-D material (Fig. 1).<sup>43</sup> When all the dimensions of a material are within the nanoscale range ( $\leq 100$  nm), such a material falls in the category of 0-D materials. Isotropic nanoparticles like spherical nanoparticles and quantum dots, nanocubes, decahedrons, octahedrons, and icosahedrons belong to this category. Materials in which two dimensions are within nanoscale range and one dimension falls outside the nanoscale are termed 1-D materials. Structures with highly anisotropic morphologies such as nanotubes, nanorods, and nanowires fall under this class. In the case of 2-D materials, one of the dimensions is within the nanoscale, and the other two are outside the nanoscale range. Such structures usually take the form of nanosheets, nanoplates, nanofilms *etc.*, which are formed in the kinetically driven regime, where the growth is allowed on two axes while restricted along the third axis. In addition to these three typical morphologies of nanomaterials, there is a fourth class known as 3-D nanomaterials, where the assembly of either one or more types of previously mentioned nanostructures happens to form a complex nanostructure. Such 3-D nanostructures display properties similar to those of their 1-D or 2-D components.

**2.2.1 0-D nanomaterials.** The 0-D nanomaterials have the lowest dimensionality and hence have sizes within 100 nm in all three dimensions, leading to the highest surface-to-volume ratios and quantum confinement effects. The shape of the resulting nanostructures is spherical or quasi-spherical. The 0-D nanomaterials can further be broadly sub-classified based on the chemical composition of the nanomaterials, such as carbon-based, inorganic material-based, and organic polymer-based nanomaterials. Isotropic spherical nanoparticles or faceted nanostructures of metals such as silver, gold, and platinum can be easily prepared by seed-mediated growth or the polyol synthesis procedure.<sup>44</sup> The carbon-based nanomaterials include graphene quantum dots, fullerenes, and carbon quantum dots. Quantum dots (QDs) are a special class of semi-



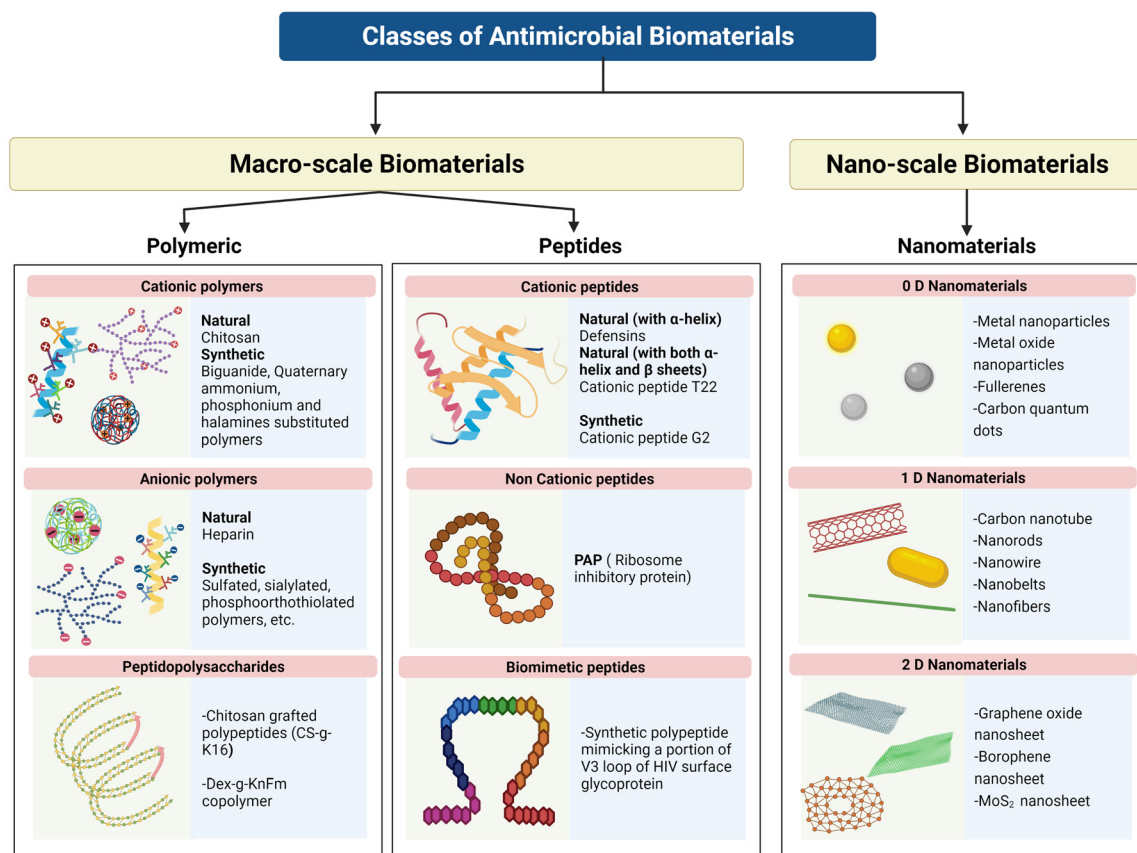


Fig. 1 Schematic showing different classes of antimicrobial biomaterials.

conductor nanomaterial ranging between 1 and 10 nm in diameter, and having electronic motion confined in all three dimensions. QDs show photoexcitation and can generate reactive oxygen species (ROS), and are excellent for photodynamic therapy to kill microorganisms or in cancer therapy.<sup>45,46</sup> Quantum dots are also claimed to be potential candidates to treat viral infections. Even in the case of COVID 19, some of the QDs have shown antiviral activity.<sup>45</sup> Other carbon-based nanoparticles (graphene quantum dots, C-dots, and fullerenes) also have inherent antimicrobial activity and can be functionalized based on the method of fabrication.<sup>47,48</sup>

**2.2.2 1-D nanomaterials.** The 1-D nanomaterials comprises nanowires, nanorods, nanotubes, nanobelts, and nanofibers, and have elongated structures in one dimension. The 1-D nanomaterials can be subclassified, based on the chemical composition of the nanomaterials, into organic and inorganic. Carbon nanotubes (CNT) are the most recognizable organic 1-D nanomaterials and find use in applications ranging from biomedical research, such as drug delivery, to consumer products such as displays, integrated circuits, lithium batteries, solar cells, and fuel cells.<sup>49</sup> CNTs have been reported to have strong antibacterial effects through a combination of chemical and physical mechanisms.<sup>50</sup> Nanorod structures of several noble metals (Ag, Au, Pd, Pt, Cu), several transition metal oxides, and a large number of groups III-V and II-VI binary

and ternary nanowires have been reported.<sup>51–54</sup> These nanostructures are effective against a broad spectrum of microorganisms, including the drug-resistant ones.

**2.2.3 2-D nanomaterials.** The development of 2-D nanomaterials began with the exfoliation of graphene in 2004 by Dr Geim and Dr Novoselov.<sup>55</sup> The 2-D nanostructures are composed of nanosheets which have a thickness of at least a few atomic layers, leading to weak van der Waals forces and in-plane bonding. Apart from graphene, the transition metal dichalcogenides, phosphorene, borophene, transition metal oxides, carbides and nitrides, metal oxides, hexagonal boron nitride, graphitic carbon nitride, perovskites, niobates, MXenes, and silicates are being explored for the synthesis of ultra-thin 2-D nanomaterials.<sup>56–58</sup> In recent years, 2D materials have emerged as one of the most promising antimicrobial biomaterials, with potent activities against a wide variety of bacteria and viruses.<sup>59,60</sup>

## 3. Antimicrobial mechanisms of macroscale biomaterials

### 3.1 Mechanism of antibacterial action of AMPs

Various studies from the last few decades have shown that the mode of action of antimicrobial peptides can be broadly classified into three major sub-types, which include pore-forming

mechanisms of membrane damage, non-pore-forming mechanisms of membrane damage, and mechanisms that target intracellular processes.

### 3.1.1 Pore-forming mechanisms

(a) *Barrel stave model*. When an AMP comes into contact with a phospholipid bilayer it forms an amphiphilic secondary structure of  $\alpha$ -helices and causes augmentation in the interfacial region of the membrane. This results in the creation of a void in the hydrocarbon tail region, which leads to generation of a positive curvature strain and membrane thinning on the opposite side.<sup>61</sup> Following this, the AMP vertically inserts itself into the phospholipid bilayer, creating a closely compact pore in which the hydrophobic residues of the peptide remain in close contact with the hydrophobic interior of the bilayer (Fig. 2a).<sup>62</sup> In 1991, Sansom *et al.* reported that Peptaibols, peptides with aminoisobutyric acid residues with C-terminal alcohol, showed antibacterial properties following the barrel stave model.<sup>63</sup>

(b) *Toroidal model*. Unlike the barrel stave model, in the toroidal model the pore lining is formed between the polar residues of the AMPs and the polar head groups of phospholipids (Fig. 2b). In view of this fact, not only can small molecules and ions pass through these pores but also phospholipid itself can pass through these pores, and can even flip-flop at high speed.<sup>64</sup> It has also been observed that a part of the peptide itself can translocate inside the phospholipid bilayer. In 1996, this model was first established during the study of magainin-induced membrane pores,<sup>65</sup> where at high magainin concentrations water-filled cavities were formed which looked like ‘worm-holes’. Hence, this model is also known as the Worm-hole model.

(c) *Disordered toroidal pore model*. Molecular dynamics simulations have shown that while interacting with dipalmitoyl-phosphatidylcholine (DPPC) membranes, Magainin H2 causes more random pore formation at multiple places through the inward twisted conformation of membrane phospholipids. Such pores are referred to as disordered toroidal pores, where one or two peptides can be present in the pore interior, while the rest of the AMPs remain in the pore lining<sup>66</sup> (Fig. 2c).

(d) *Carpet model*. At high peptide-to-lipid ratio and in the presence of negatively charged phospholipids, some AMPs tend to accumulate together and adsorb at high concentrations on the phospholipid bilayer, resembling a carpet.<sup>61</sup> As a result of this typical arrangement, the electrostatic repulsive forces existing between positively charged peptides get reduced or diminished to a large extent, which ultimately leads to lysis of the membrane (Fig. 2d).<sup>67</sup> This model was first proposed by Shai in the year of 1996 while explaining the antibacterial action of MOA of mammalian cecropin P1 on model membranes.<sup>68</sup>

(e) *Detergent-like model*. This model is very much applicable to explain the activities of amphiphilic peptides on membranes. Similar to detergents, amphiphilic peptides form micelles with the lipid bilayer at concentrations above their critical micelle concentration (CMC) and form aggregates (Fig. 2e). This property greatly depends on the detergent/AMP-to-lipid ratio. For example, in the presence of very little detergent there is no negative effect on the membrane; rather, it stabilizes it. However, at intermediate concentrations it starts to form small transient pores, which at high concentrations of the detergent results in disintegration of the lipid bilayer. AMPs can exist both as monomers and oligomers. When present as oligomers, AMPs may act like detergent and form micelles with the lipid bilayer, causing disintegration, loss of membrane barrier, dissolution of the electrostatic gradient across the membrane, interference in energy metabolism of living cells and finally loss of cytoplasm and its constituents.<sup>67</sup> Cecropin B is a very good example of an AMP showing bactericidal activity through this detergent-like model.<sup>69</sup>

(f) *Interfacial activity model*. The core of the lipid bilayer membrane is one of the most hydrophobic microenvironments present in nature. It acts as a permeability barrier for polar or charged solutes, but itself is surrounded by two bilayer interfacial zones named “zones of tumultuous chemical heterogeneity”.<sup>70</sup> When a peptide molecule disturbs the hydrophobic core region of a phospholipid bilayer by interfering in the interfacial region of the bilayer, it causes local rearrangements in vertical lipid packing. As a result of this, separation of the

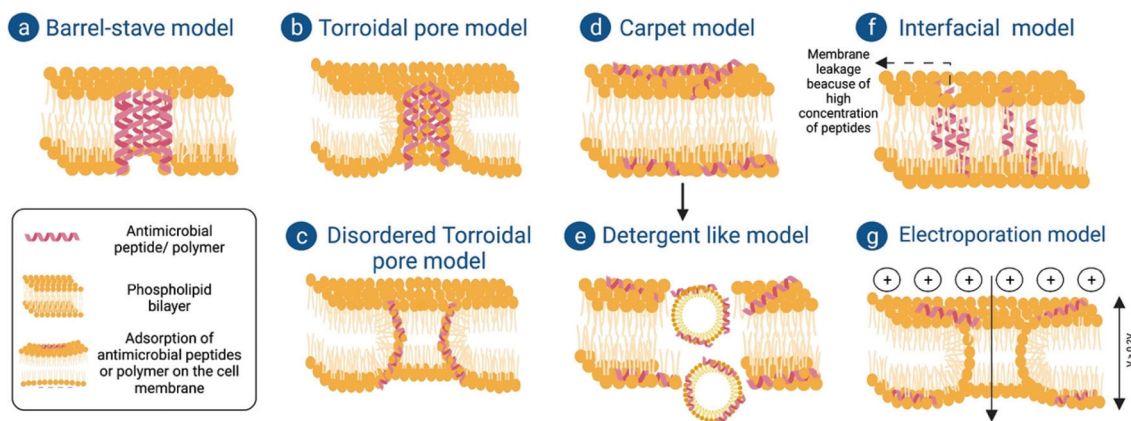


**Fig. 2** Schematic of different models showing "pore-forming" mechanisms of membrane damage by antimicrobial macromolecules. (a) Barrel-stave model, (b) Toroidal pore model, (c) Disordered Toroidal pore model, (d) Carpet model, (e) Detergent like model, (f) Interfacial model and (g) Electroporation model.

interfacial groups takes place, and the hydrocarbon core region is lost (Fig. 2f). This can be described as a peptide's interfacial activity.<sup>25</sup> This model is mainly dependent on the amino acid sequence of the AMP rather than its peptide structure. It requires AMPs to have "imperfect amphipathicity", where instead of a large hydrophobic segment, such segments are present in the AMP structure which are large enough to traverse the phospholipid bilayer but are interrupted by at least polar residues like arginine or lysine. Such types of AMP translocate through the bilayer along with lipid molecules even at low peptide concentrations, and at higher concentration this causes membrane leakage.<sup>25</sup> AMPs like cyclic AMP Rhesus theta Defensin, helical AMP Xenopus Magainin 2, globular peptide Human  $\alpha$ -defensin and Human  $\beta$ -defensin, *etc.* show membrane disruption through the interfacial activity model, independent of their structures but based on their amino acid sequences.

(g) *Electroporation model.* It is observed that when highly charged molecules bind with the phospholipid bilayer, electrostatic potential is developed on the membrane. If the electrostatic potential is at least 0.2 V across the phospholipid bilayer, then it can create pores across the membrane without changing its conformation (Fig. 2g). Through these pores small molecules and even the peptide itself can pass, as these pores have sizes of 2–4 nm in diameter.<sup>71</sup> Miteva *et al.* reported such a mechanism of action in a single highly charged  $\alpha$ -helical segment of NK-lysin.<sup>72</sup>

### 3.1.2 Non-pore-forming mechanisms

(a) *Membrane thinning model.* When peptides are aligned on the surface of the outer bilayer, they interact with the polar head groups of the phospholipid bilayer and expand the local area. To keep the volume constant, the length of the acyl chains decreases, hence causing membrane thinning (Fig. 3a). The thinning of the membrane depends on the elastic constants of the bilayer, which can extend over a range of approximately 40 Å.<sup>73</sup> At a sufficiently high peptide concentration, the deformations created by each peptide will overlap and will create a uniform thinning of the membrane. Therefore, the overall thin-

ning of the membrane is proportional to the peptide-to-lipid ratio. Peptides which are not able to form pores and insert into the bilayer, such as Mag2, GS, and BP100, follow this mechanism for their antimicrobial activity.<sup>74</sup>

(b) *Non-lytic membrane depolarization.* There are certain peptides which can cause bacterial membrane damage by depolarization without forming actual ion channels or pores. Huang *et al.* showed that when a cyclic lipopeptide daptomycin binds with the bacterial phospholipid bilayer it inserts its acyl fatty acid chain into the bacterial membrane in a calcium-dependent manner, thereby causing oligomerization of membrane proteins to form ion channels or pores, but this phase is very transient and recovers back quickly.<sup>75</sup> Through these pores potassium ions leak, which causes a reduction in membrane potential from  $-165$  mV to  $-100$  mV; as a result of this, the electrochemical gradient-induced proton motive force, which is a prerequisite for adenosine triphosphate synthesis, gets disrupted (Fig. 3b). Adenosine triphosphate plays an important role in many intracellular processes like active transport of nutrients, synthesis of peptidoglycan precursors and many more cell signaling pathways.<sup>76</sup>

(c) *Non-bilayer intermediate model.* A few peptides follow another non-pore-forming pathway whereby they become internalized inside the cell without disrupting the membrane integrity (Fig. 3c).<sup>77</sup> Powers *et al.* reported that an antimicrobial peptide, polyphemusin, translocates the lipid bilayer without breaking the integrity of it. Firstly, it interacts with the membrane mainly with the negatively charged polar head groups and partially enters the membrane. After insertion of a sufficient number of peptides, they aggregate and produce a negative curvature stress which forms a non-bilayer intermediate with the remaining peptides inside the hydrophobic core. Finally, this non intermediate core disrupts and the peptides in it redistribute themselves in the outer and inner leaflets of the phospholipid bilayer.<sup>78</sup>

(d) *Anionic phospholipid clustering model.* Cationic peptides can attach with the negatively charged polar head groups in

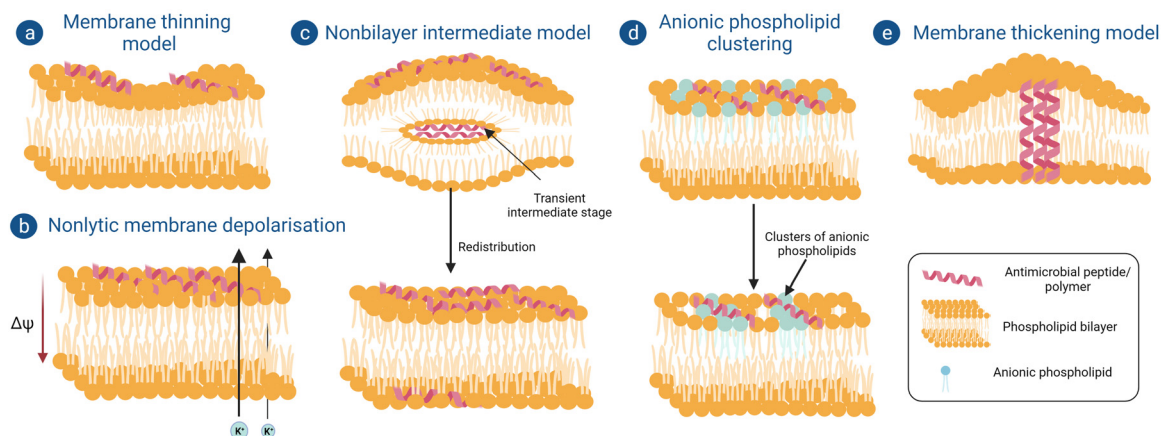


**Fig. 3** Schematic of different models showing "non-pore-forming" mechanisms of membrane damage by antimicrobial macromolecules. (a) Membrane thinning model, (b) Nonlytic membrane depolarization, (c) Nonbilayer intermediate model, (d) Anionic phospholipid clustering and (e) Membrane thickening model.



the bacterial membrane and form clusters of anionic phospholipids (Fig. 3d). This charge clustering sometimes leads to the formation of transient pores in the membrane and causes infringement of the membrane barrier, leading to leakage of cytoplasmic contents and membrane depolarization. Such mechanism of antimicrobial action was reported for C12K-7 $\alpha$ 8 peptide.<sup>79</sup>

(e) *Membrane thickening model.* While studying the antimicrobial action of an  $\alpha$ -helical antimicrobial peptide, peptidyl-glycyl-leucine-carboxamide (PGLa)<sup>80</sup> on a phosphatidyl glycerol model membrane, it was observed that initially they were not able to insert themselves completely inside the membrane. Rather, to match the hydrophobic part of the peptide, hydrophobic tails of the phospholipids shifted towards it, resulting in a local thickening of the membrane and causing bacterial membrane deformation (Fig. 3e). But after crossing a certain peptide concentration, these peptides start to insert themselves into the membrane vertically or at an oblique angle, eventually forming pores like the barrel stave model or toroidal model and causing bacteriolysis.

### 3.1.3 Mechanisms that target intracellular processes

(a) *Cell wall synthesis.* There are antimicrobial peptides which target various intracellular pathways of the microorganism. Lantibiotics are a group of lantionines with antimicrobial peptides against Gram-positive bacteria. Among these Mersacidin is the smallest lantibiotic with antimicrobial

properties. Heike *et al.* reported that the antimicrobial activity shown by this peptide does not involve pore formation; rather, it interferes with peptidoglycan synthesis. In the presence of Mersacidin, glucose uptake is significantly reduced thereby leading to a reduction in the synthesis of cell wall-specific D-amino acids (Fig. 4). However, this does not have any effect on DNA, RNA or protein synthesis. The study suggested that Mersacidin reduced peptidoglycan width from 30–34 nm to 17–20 nm. This caused bacterial cells to rupture because of osmotic pressure. Further, it was also shown that this lantibiotic can reduce overall teichoic acid content in the treated cell.<sup>81</sup>

(b) *Cell division.* A few antimicrobial peptides result in the generation of filamentous bacterial cells, which can be a direct consequence of inhibition of various intracellular pathways like improper chromosome segregation, inhibition of septum formation, inhibition of DNA replication or SOS induction. Salomón *et al.* reported that Microcin J25, a 20 amino acid peptide, results in the formation of filamentous bacterial cells through blocking the septation process of cell division (Fig. 4). In the presence of the antimicrobial peptide, microscopically it was observed that *E. coli* cells increased in length until they took on a long aseptate filamentous structure. In parallel, cell mass was also increasing which was a clear indication of the increase in bacterial cell length because of inhibition of cell division. It was also found that even in the presence of proph-

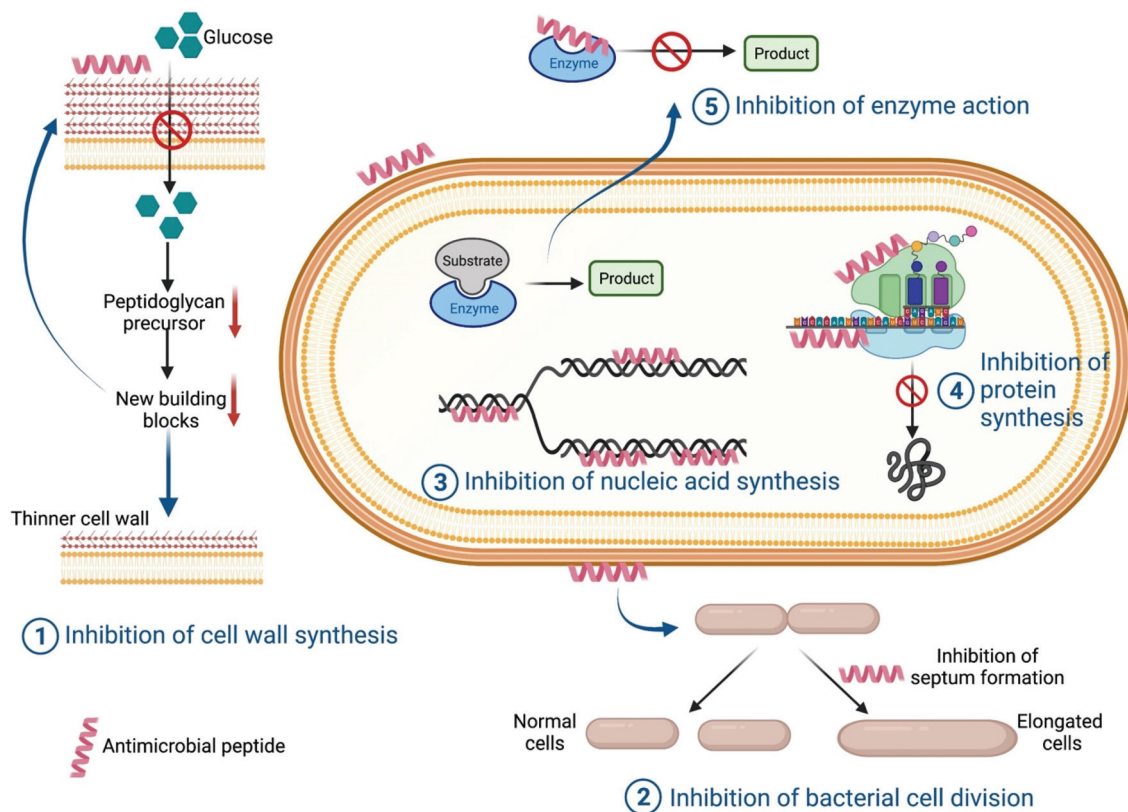


Fig. 4 Schematic showing different mechanisms of intracellular targeting pathways by antimicrobial peptides.

age induction, there was a relatively low phage titer in AMP-treated cells, which suggested it was a non-SOS dependent pathway and hence showed only a bacteriostatic effect.<sup>82</sup> A similar effect was also observed for the peptide dipterin in *E. coli* cells.<sup>83</sup>

(c) *DNA/RNA synthesis.* Nucleic acids are a major component of any cell. Both DNA replication and RNA transcription are complex and multistep processes which involve different enzymes and proteins. Hence each step, including the components, can be a potential target for antimicrobial peptides. There are a few AMPs which have structural similarities with proteins that have DNA or RNA-binding domains. Such AMPs bind with the respective nucleic acids and inhibit their function. They can also inhibit any enzymes involved in replication, transcription or post transcriptional pathways (Fig. 4). Buforin II is an antimicrobial peptide which has structural homology with the N-terminal fragment of the DNA-binding protein histone H2A, and binds with the DNA fragment to interrupt DNA or RNA metabolism.<sup>84,85</sup>

(d) *Protein synthesis.* After DNA replication and mRNA transcription, translation of mRNA takes place *via* the 70S ribosome in the case of prokaryotic cells, whereas in eukaryotic cells 80S ribosomes are required for protein translation. Hence this is a very good potential target for antimicrobial activity. Besides, inhibition of any intermediate step can halt protein synthesis (Fig. 4). Bac-7, a 60-residue peptide, can be internalized by inner membrane protein SbmA of *E. coli* and shows antimicrobial action by targeting the bacterial ribosomes.<sup>86</sup> Inhibition of protein synthesis can be targeted by many other antimicrobial peptides.<sup>87,88</sup>

(e) *Enzymatic action inhibition.* For a living cell, cellular metabolism is an important process which includes various overlapping and independent biochemical reactions. The total system is like an orchestra, so inhibition of any one reaction can cause the whole cellular system to diminish. Therefore, cellular biochemical reactions are a very common target for antimicrobial peptides. UDP-*N*-acetylglucosamine acyltransferase enzyme is the enzyme of the first step of lipid A synthesis, which is one of the main components of Gram-negative bacteria's outer membrane. A penta-decapeptide (Peptide 920) targets this enzyme and has a very high affinity towards the active site of this enzyme, thus preventing its catalysis of lipid A. As a result, an incomplete membrane structure will be formed, which is lethal for Gram-negative bacteria<sup>89</sup> (Fig. 4).

### 3.2 Mechanism of antiviral action of antiviral peptides

In today's scenario, viral outbreak and resistance are the biggest global health and economic concerns. This situation acts as a positive stimulus for the search for new antivirals. Antivirals do not always have the property of directly killing or destroying the viruses; rather, in most cases they act by disrupting the machinery of viral infection.<sup>90</sup> The process of viral infection involves (i) attachment of virus to the host cell membrane through specific ligand–receptor interactions between the virus and its target cell, which is then followed by (ii) penetration or internalization of the virus inside the host cell. Once

inside the host, (iii) the virus hijacks the genetic machinery of the host to replicate its genetic material, followed by its translation into viral proteins. Once the viral genome has been copied and necessary structural components have been synthesized, (iv) packaging of the viral genome into protein structures takes place to form virions, which finally fuse with the host cell membrane to bud-off from the cell surface and get released as progeny viruses. Each stage of this replication machinery can be a potential target for any antiviral biomaterial.

**3.2.1 Cationic antiviral peptides.** Mammalian cells usually express highly sulfated branched glycoproteins called heparan sulfate proteoglycans (HSPGs) on their surface, which are recognized by positively charged viral proteins for initial low affinity interaction between the virion and the host cell. Cationic peptides are such peptides with positive charge which can interact with negatively charged HSPGs and inhibit virus attachment with the host cell. Therefore, the main antiviral mechanism shown by cationic peptides is inhibition of virus attachment to host cells by itself binding to host surface receptors.<sup>91–93</sup> Cationic antiviral peptides can be of two types, naturally occurring cationic antiviral peptides and synthetic cationic peptides.

**i Naturally occurring antiviral peptides:** naturally occurring peptides with cationic residues show a similar effect but their amphipathic  $\alpha$ -helical conformation and  $\beta$ -sheet structures also play important roles. On the basis of their mode of action, they can be classified as follows:

1. *Inhibition of viral attachment on the host cell:* lactoferricin, an  $\alpha$ -helical cationic peptide containing 21 amino acids, shows antiviral activity by preventing viral attachment to host cells.<sup>94,95</sup> It was suggested that lactoferricin binds with the heparan sulfate proteoglycans (HSPGs) present on the mammalian cell surface and therefore blocks viral attachment to the host cell.<sup>96</sup>

2. *Inhibition of viral entry inside the host cell:* cationic peptide T22, which has  $\beta$ -sheet conformation, shows antiviral activity against HIV-1, but rather than the cationic moiety,  $\beta$ -sheets play a more important role here by interrupting binding of CXCR4, a T-cell receptor which is utilized by the viral particle for entry into the host cell.<sup>97,98</sup>

3. *Inhibition of viral cell fusion with the host cell:* another cationic antiviral peptide obtained from bee venom is Melittin. It was reported that this peptide is able to inhibit Herpes simplex viral infection and Junin virus infection by inhibiting viral particle fusion with the host cell membrane.<sup>99</sup>

4. *Inhibition of viral replication:* it was reported by Wachinger *et al.* that cationic antiviral peptide Cecropin and also Melittin were able to inhibit HIV-1 infection by suppressing activity of the HIV Long terminal repeat.<sup>100</sup>

**ii. Synthetic peptides:** Krepstakies *et al.* reported that 20 amino acid-long peptides containing lysine and arginine residues can successfully inhibit a broad spectrum of viral infections including Human Immunodeficiency Virus (HIV) type1, Herpes Simplex virus (HSV) type 1 and type 2, Hepatitis B virus (HBV) and Hepatitis C virus. Their study showed that the anti-

viral action of these peptides is observed when used prior to viral infection. The mechanism of action exhibited by these peptides thus mainly involves inhibition of viral attachment to the host cells before membrane fusion.<sup>101</sup> Similar results have been shown in studies with 12 amino acid-containing cationic peptide G2 against HSV-2 viral infection. This peptide was able to inhibit not only viral attachment but also viral fusion with the host cells.<sup>102</sup>

### 3.2.2. Naturally occurring non-cationic antiviral peptides.

There are many naturally occurring antiviral peptides which can exert their antiviral activity by different mechanisms of action. American pokeweed antiviral protein PAP is a ribosome inhibitory protein. It was reported that PAP shows antiviral activity against plant tobacco mosaic viruses by inhibiting their protein synthesis.<sup>103</sup>

**3.2.3. Biomimetic peptides.** These are the peptides which mimic structures that are requisite for viral and host cell binding. Hence, again the mechanism of action followed by this type of antiviral peptide is inhibition of virus attachment with the host cell. A synthetic polypeptide that can mimic a portion of the V3 loop of HIV surface glycoproteins was found to inhibit viral attachment to human CD4+ cells.<sup>104</sup>

## 3.3 Mechanism of antibacterial action of polymeric biomaterials

**3.3.1 Cationic polysaccharides.** Cationic polysaccharides are a group of molecules which mimic antimicrobial natural host defense peptides. They can be natural as well as chemically modified. Polysaccharides are one of the most abundant molecules present in the environment and many of them have intrinsic antimicrobial properties, but cationization of them helps to increase their antimicrobial potency, hence making them a potential antimicrobial agent. Cationic antimicrobial polysaccharides mainly target the negatively charged outer envelope of bacterial cells, which is why they are also known as membrane active agents. Among all cationic polysaccharides, the most exploited is chitosan. It is a deacetylated form of chitin. The mechanism of action exerted by chitosan depends on three major factors: (1) electrostatic interaction, (2) hydrophobic interaction and (3) chelating effect. The main property which provides the antimicrobial activity to chitosan is its positive charge coming from the amino groups present in its structure. In acidic conditions, when pH is less than chitosan's  $pK_a$  value, amino groups get protonated and become  $-NH_3^+$ , which is responsible for its cationic characteristic. As a result, chitosan interacts with the negatively charged membranes of both Gram-positive and Gram-negative bacteria through electrostatic interactions and inhibits bacterial growth. It is also observed that high molecular weight chitosan molecules may not be able to internalize themselves; rather, such polymers prefer to deposit as a dense layer on the outer surface of the bacterial cell and prevent the supply of nutrients and oxygen, which again results in bactericidal action. Lastly, divalent ions also play a huge role in both Gram-positive and Gram-negative bacteria, starting from maintaining cellular integrity to various essential enzymatic cations. Chitosan can

chelate the divalent ions present on the cellular surface and inhibit bacterial growth.<sup>105</sup>

A moderately different mechanism has also been found in the case of another cationic polysaccharide, namely quaternized pullulan.<sup>106</sup> Pullulan is a fungal exopolysaccharide secreted by the black fungus *Aureobasidium pullulans*. Pullulan itself does not have any antibacterial activity; however, cationization of this polysaccharide through the introduction of quaternary ammonium groups into the polysaccharide backbone results in the creation of a highly potent bactericidal agent. Quaternized pullulan has been observed to exert its bactericidal action against both Gram-negative and Gram-positive bacteria through a typical non-pore-forming pathway, which does not involve the formation of classical "pores" for disrupting bacterial membranes.<sup>106</sup> Such a mechanism of action is more common for antimicrobial peptides than for antimicrobial polysaccharides. Both atomistic MD simulations and *in vitro* experiments showed that interaction of the cationic pullulan with the exposed negatively charged polar head groups of the bacterial cell membrane occurs *via* electrostatic interactions, which results in the polymers getting tightly adsorbed on the outer membrane surface of the bacteria. Subsequently, this leads to the clustering of anionic phospholipids into domains in the bacterial membrane (Fig. 5). These negatively charged clusters or domains cause a difference in the packing of the hydrophobic tails of phospholipids, which ultimately causes a difference in fluidity on one leaflet of the membrane. As a result, the properties of the other leaflet are also affected, a phenomenon known as interleaflet coupling. This phenomenon has the ability to create transient pores in the membrane through which water molecules and ions can pass, thereby resulting in depolarization of the membrane. A combined effect of anionic lipid clustering and membrane depolarization makes the bilayer weak over time, which ultimately results in physical disruption of bilayer integrity and cell death.

**3.3.2 Cationic synthetic polymers.** Depending on the chemical groups used for their modification, cationic synthetic polymers can be classified into three main categories as follows:

i. *Biguanide polymers:* polyhexamethylene biguanide chloride (PHMB) is the first antimicrobial polymer whose interaction was studied against Gram-negative bacteria *E. coli* and a model phospholipid membrane. The study suggested that after interaction of the polymer with the cell membrane a domain of acidic phospholipids is created that compromises the integrity of the outer membrane in the case of Gram-negative bacteria. First, it gets adsorbed on the outer membrane and compromises its integrity so that it can internalize further and interact with the inner membrane. This makes the membrane more porous, which results in leakage of  $K^+$  ions. At this stage, the polymer mainly inhibits bacterial growth. However, complete loss of membrane function ultimately leads to cell lysis.<sup>14,107</sup> 4-(2-Hydroxyethyl)aniline hydrochloride(II), 4-(2-hydroxyethyl) phenyl dicyandiamide(III), N1-4-(2-acryloyl oxyethyl) phenyl-A5-4-chlorophenyl biguanide hydrochloride(VI)



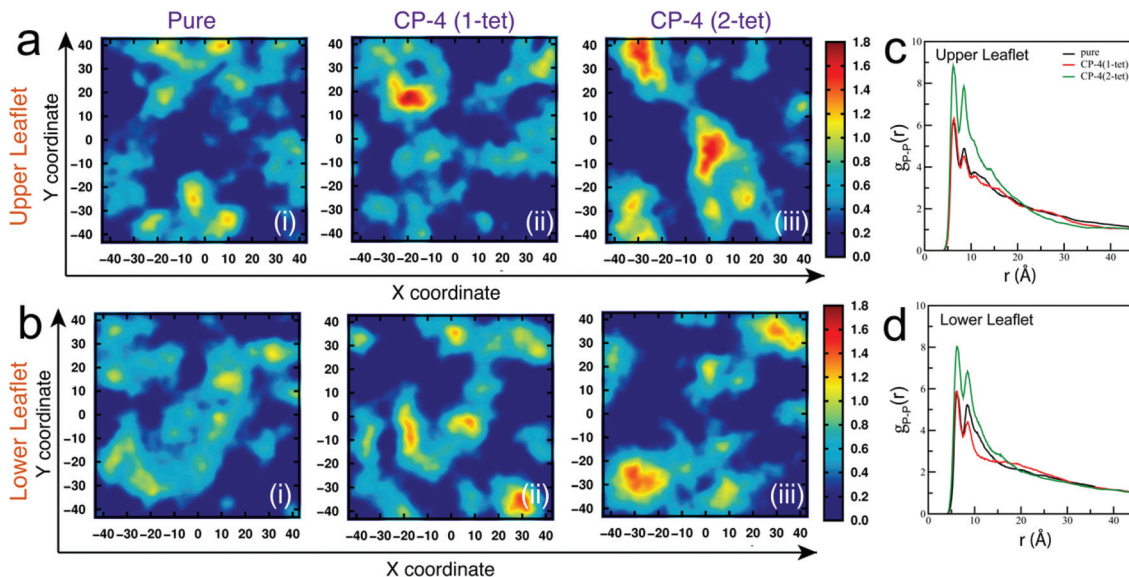


**Fig. 5** Anionic lipid clustering induced by quaternized pullulan. Two-dimensional number density plots for DOPG lipids in  $xy$ -plane orthogonal to membrane normal with subsequent addition of CP-4 molecules (a) upper leaflet and (b) lower leaflet. The units of  $x$  and  $y$  coordinates and number density are Å and Å<sup>-2</sup>, respectively. Radial distribution function for P–P atomic pairs of DOPG lipid head groups for (c) upper leaflet (d) lower leaflet. Reproduced with permission.<sup>106</sup> Copyright 2022, Royal Society of Chemistry.

*etc.* are chemically synthesized biguanide polymers which also show antimicrobial activity against both Gram-positive and Gram-negative bacteria.<sup>108</sup>

ii. *Quaternary ammonium or phosphonium polymers*: in the case of quaternary ammonium or phosphonium polymers, the basic mechanism of action is similar. Because of the presence of cationic charge, the polymers get absorbed on the outer envelope and damage the outer membrane mainly through non-pore-forming pathways of membrane destruction (Fig. 3). In the majority of cases, the polymers exert their membrane-damaging action without themselves penetrating the membranes.<sup>109,110</sup> A copolymer of 2-chloroethylvinyl ether and vinylbenzylchloride with immobilized phosphonium ions showed a similar bactericidal effect on both Gram-positive *Staphylococcus aureus* and Gram-negative *E. coli*.<sup>111</sup> Another copolymer (PEB-*b*-PDMAEMA), which is copolymerised with octyl bromide, was synthesized by Lenoir *et al.* by quaternization of amino groups of poly(ethylene-*co*-butylene)-*b*-poly[2-(dimethylamino)ethyl-methacrylate]. This copolymer also showed antibacterial activity against *E. coli*.<sup>112</sup> A highly hydrophilic and biocompatible monomer hydroxyethylmethacrylate (HEMA) and polyethylene glycol methyl ether methacrylate (PEGMA) were incorporated in quaternized poly(vinylpyridine) (PVP) *via* copolymerization with 4-vinyl pyridine. This copolymer has shown much better antibacterial activity against *E. coli* than normal PVP.<sup>113</sup> A series of tributyl(4-vinylbenzyl) phosphonium salts with different counter anions and corresponding polymers have shown antibacterial activity against *S. aureus* where the antibacterial activity emerged from the counter anions.<sup>114</sup> Those counter anions which were tightly bound with the phosphonium ions showed relatively less anti-

bacterial activity than the counter anions which completely dissociated into free ions.

iii. *N-Halamine polymers*: this is a group of bactericidal polymers where *N*-halamine precursors are covalently bonded with nitrogen atoms of the targeted polymer. Upon halogenation they are converted to *N*-halamine structures which provide stability to the polymeric structure and allow slow release of free halogens in the environment to show bactericidal effect. *N*-Halamine polymers have broad-spectrum antibacterial property. Here, not the overall polymer but the free oxidative halogen along with its bound compound (thiol groups or amino groups) comes into direct contact with bacterial cells and results in cellular inactivation.<sup>115,116</sup> A recent study shows that *N*-halamine acrylamide monomer, a hydantoin acrylamide (HA), is produced by forming a hydantoin ring from the ketone moiety of a secondary amide monomer, *N*-(1,1-dimethyl-3-oxobutyl) acrylamide (DA). HA was copolymerized with a siloxane monomer (SL) using different feed ratios, and this copolymer can be used as an antimicrobial coating on fabric.<sup>117,118</sup> Kocer *et al.* reported another series of water-dispersible biocidal polymers which can be used as antimicrobial paints. These were synthesized by copolymerization of the hydantoin acrylamide and sodium salt of 2-acrylamido-2-methylpropane sulfonic acid.<sup>119</sup>

**3.3.3 Peptido-polysaccharides.** Both Gram-positive and Gram-negative bacteria have cell walls made of peptidoglycans, which is a layer consisting of polysaccharides and short peptide chains. This is absent in eukaryotic cells. So, conjugates of peptide and polysaccharides which mimic the structure of the peptidoglycan layer act as broad-spectrum antimicrobial agents by targeting the bacterial cell wall. Such

mimics are called peptido-polysaccharides. There is a series of cationic polymers such as chitosan-grafted polypeptides (CS-*g*-K<sub>16</sub>),<sup>120</sup> a copolymer (Dex-*g*-K<sub>n</sub>F<sub>m</sub>) made of methacrylate-ended poly(lysine-random-phenylalanine) and a thiolated polysaccharide dextran<sup>121</sup> which mimic the peptidoglycan layer and show broad-spectrum antimicrobial activity. They first interact with the anionic bacterial cell wall by electrostatic interactions and increase the permeability of this layer. After diminishing the integrity of the cell wall, these polymers internalize into the cytoplasm through the cell membrane, resulting in bacterial cell lysis because of osmotic imbalance. So, the mechanism of action of such polymers is through increasing cellular permeability, resulting in “leaky” cells which eventually rupture.

### 3.4 Mechanism of antiviral action of polymeric biomaterials

Polymers, because of their high molecular weight and repetitive structure, have emerged as a promising class of antiviral biomaterial. Polymeric biomaterials can be divided into anionic and cationic polymers, depending on the type of charge they carry on their surface.

#### 3.4.1 Mode of action of anionic polymers

(a) *Sulfated polymers.* Sulfated polymers can be both polysaccharides and non-glycosylated polymers.

i. **Sulfated polysaccharides:** depending on the polymeric subunit and virus particle, different antiviral mechanisms have been observed.<sup>122,123</sup>

*Virucidal activity:* some polysaccharides because of their negative charge can directly show a virucidal effect on some envelope viruses by altering the envelope proteins of the viruses so that they are no longer available for interaction with the host cells, hence reducing their virulence. Carrageenan is a sulfated polysaccharide whose  $\lambda$ -type can firmly attach to the Herpes Simplex virus (HSV) and cause structural changes in the viral glycoprotein gB and gC, thereby inactivating the virus for further interaction with host cells.<sup>124,125</sup> Chitosan and its oligosaccharides can also have direct virucidal activity against some human enteric viral surrogates.<sup>126,127</sup>

*Inhibition at attachment stage:* this is the first stage in viral infection, when virus particles interact with the host cells through their membrane proteins and bind with specific receptors present on the host cell surface. At first this interaction is reversible, but slowly irreversible interaction develops. Various antiviral polymers are available which target the viral membrane proteins so that they are not able to bind with the host cell receptor, or polymers can also bind with the host cell receptors thereby making these receptors no longer available for the viral proteins. Dextran sulfate and heparin were found to interfere with the interaction between HIV glycoprotein gp120 and CD4<sup>+</sup> antigen receptors present on the T lymphocytes.<sup>128–130</sup> There are many more polymers like sulfated galactan from red algae,<sup>131</sup> chitosan derivatives,<sup>132</sup> and fucoidan from brown algae<sup>133–136</sup> which show antiviral activity using this mechanism.

*Inhibition at internalization and uncoating:* viral internalization and uncoating occurs after the adsorption step.

Internalization and uncoating usually occurs in a stepwise manner though in an allosteric way, but they can also take place simultaneously in some viruses.<sup>137</sup> Viral internalization mainly occurs through a vesicular endocytic pathway where viral particles are transported to endosomes or any targeted subcellular organelles through cytoplasm inside a vesicle.<sup>138</sup> Some antiviral polymers can block any of the above steps. Kim *et al.* showed that p-KG03, a sulfated polysaccharide obtained from *Gyrodinium impudium*, can inhibit Influenza A viral infection if administered during or within 6 h of viral infection. This suggests that the polymer interferes primarily at the adsorption stage and also in the internalization of the virus inside the host cell.<sup>139</sup> There are many other polysaccharides, like Carrageenan, which also follow this mechanism against HPV<sup>140</sup> and DENV<sup>141,142</sup> viruses.

*Inhibition of viral replication and transcription:* the molecular weight of the polysaccharides plays an important role in inhibiting viral replication and transcription. Large molecular weight polysaccharides which are not able to enter the host cell show their antiviral activity at the adsorption stage; however, the low molecular weight version of the same polysaccharide which can get internalized exhibits its antiviral activity by inhibiting viral genome replication or transcription. It can also interfere in the viral protein translation process. It has been demonstrated by Wang *et al.* that the antiviral activity of Carrageenan oligosaccharide CO-1 against IAV is not at the adsorption stage. The oligosaccharide cannot even bind to the surface of host MDCK cells directly. Thus, after internalization it inhibits IAV mRNA transcription and protein synthesis.<sup>143</sup> Another such example is that of sulfated fucan, which can inhibit HIV by inhibiting its reverse transcriptase enzyme required for viral genome replication.<sup>144,145</sup>

*Indirect antiviral effect:* when a cell is infected with virus, it induces the type I interferon system, which is a host's innate antiviral mechanism and prevents viral multiplication inside the host cell. There are a few polymers which induce this host antiviral mechanism, hence indirectly showing antiviral property. A sulfated polysaccharide (SPPMG) obtained from brown algae has shown an indirect antiviral effect on HIV and HBV infection by inducing cellular and humoral immunity of the host cell.<sup>146,147</sup> There are various other polymers like  $\lambda$ -Carrageenan<sup>148–150</sup> which show a similar antiviral effect.

**3.4.2. Sulfated non-glycosylated polymers.** Various issues like poor bioavailability, short plasma half-life, and demanding synthesis process make sulfated polysaccharides a difficult choice when it comes to antiviral therapeutics. Hence, as an alternative, sulfated non-glycosylated polymers have also been synthesized.<sup>151</sup> The main mode of action exerted by sulfated non-glycosylated polymers is inhibition of viral adsorption through forming an electrostatic interaction with the viral particle. However, it has been found that such polymers can also act by inhibiting any other later stages of viral replication. The very first sulfated non-glycosylated polymer synthesized was PRO2000, a 5 kDa naphthalene sulfonate polymer which showed antiviral activity against HIV-1 by inhibiting virus attachment to the host cell membrane.<sup>152,153</sup> To increase the

antiviral property of PRO2000 against HSV-2, it was functionalized to a more complicated 16 kDa protein structure which was able to inhibit viral infection at the later stages after viral internalisation.<sup>154,155</sup>

(a) *Sialylated polymers.* Sialylated polymers can be defined as polymers having sialic acid components in their structure. This type of polymer especially works against influenza virus. The antiviral mode of action followed by these polymers is inhibition of viral attachment to the host cells.<sup>156</sup> The resistance rate of influenza virus is considerably high because the virus particle interacts with the host cell through its surface glycoprotein hemagglutinin with the sialylated glycans present on the host cells which share different properties, hence sulfonated or sulfated polymers are not highly efficient against influenza virus. The antiviral efficiency of these polymers depends on the degree of substitution, and it also increases with substitution.<sup>157,158</sup>

(b) *Phosphonothioate polymers.* Since late 1970, nucleotide and nucleoside analogs have been established as antiviral agents but viruses easily adapt to their antiviral mechanism and become resistant.<sup>159,160</sup> Synthetic oligonucleotides are promising antivirals, but to increase the *in vivo* half-life and resist nuclease attack, phosphonothioation of the phosphodiester linkages is done which provides the polymers with anionic as well as amphipathic properties, making them a potential contender for antiviral therapy. As they mimic natural nucleotides, such polymers are also known as Nucleic Acid Polymers (NAPs),<sup>161</sup> such as Adenosine 3,5'-cyclic phosphorothioate, Adenosine 5'-phosphorothiolate,<sup>162</sup> and REP2139, a phosphorothiolate polymer used against Hepatitis B virus.<sup>163</sup> The antiviral efficiency of a NAP is independent of its sequence but very much dependent on the amphipathicity and length. NAPs show a broad spectrum of antiviral activity both under *in vitro* and *in vivo* conditions.<sup>164-166</sup> The mechanism of action of these polymers is similar to that of sulfated polymers, *i.e.* it can prevent viral attachment to the host cell surface, and can inhibit later stages like viral assembly.<sup>166</sup>

### 3.4.3 Mode of action of cationic polymers

(a) *Amine-functionalized polymers.* The primary mode of action of these polymers against viruses is inhibition of viral attachment to the host cell membrane. Eudragit E100, an ammonium-functionalized polymer which is a copolymer of methyl methacrylate, *N,N* (dimethylamino) ethyl methacrylate and methacrylate in 1:2:1 composition, shows antiviral activity against a wide variety of viruses such as HSV-2, VSV, bovine viral diarrhoea virus, and Measles virus by preventing the viruses from attaching to the host cell membrane.<sup>167,168</sup> Molecular dynamics simulations suggest that cationic oligomeric-conjugated polyelectrolytes (OPEs) made of synthetic poly(phenylene ethynylene) show antiviral action against MS2 and T4 bacteriophages by strongly binding with the viral capsid *via* electrostatic interactions and van der Waals forces, which causes viral capsid destruction.<sup>169,170</sup>

(b) *Guanidine-functionalized polymers.* It has been shown that the guanidine moiety exhibits antiviral activity against both enveloped and non-enveloped viruses. So, polymers func-

tionized with the guanidine moiety show a broad spectrum of antiviral activity against Equine herpes virus type 1, Rhinotracheitis infectious bovine and Equine infectious anemia virus.<sup>171</sup> Such polymers showed antiviral properties only when administered prior to infection, thus suggesting that the mode of action of these polymers was again inhibition of viral attachment to the host cells by itself binding to the phospholipids of the host cell membrane.<sup>171</sup>

## 4. Antimicrobial mechanisms of nanoscale biomaterials

In this section, we present a comprehensive and general outline of the possible mechanisms involved in the antibacterial and antiviral action of nanostructures of different dimensionalities such as nanoparticles, nanotubes and nanosheets, and try to provide an overview of the possible sequence of events that might take place when a bacterial cell or a virus interacts with a specific class of nanostructure, ultimately leading to its death. Different factors such as diameter, length (short *vs.* long), degree of oxidation, surface chemistry, electronic structure (metallic *vs.* semiconductor), as well as microbial strain and morphology have been taken into consideration in understanding the mechanism of action of these nanostructures. We have restricted our discussion to the inherent antibacterial and antiviral effects of pristine nanostructures of different dimensions without any antimicrobial surface functional agents such as surfactants, polymers or loaded with any other biocidal agents.

### 4.1 Mechanism of antibacterial action of 0D nanoparticles

0D nanoparticles have been widely used as antibacterial agents. Among the different types of nanoparticle explored as antibacterial agents, metal (Ag, Au, Cu) and metal oxide (Cu<sub>2</sub>O, CuO, ZnO, MgO, TiO<sub>2</sub>, Al<sub>2</sub>O<sub>3</sub> *etc.*) nanoparticles have been studied the most. Carbon dots too have emerged as promising antibacterial agents. In the following section, we discuss how these 0D nanoparticles interact with bacteria and exert their antibacterial action.

**4.1.1. Direct physical contact and membrane damage.** The initial step towards the antibacterial action of the majority of the nanoparticles studied so far is the establishment of direct physical contact with the bacterial cell wall and membrane, leading to alterations in the membrane structure, permeability and transport activity. Attachment or adherence of nanoparticles on the surface of the bacterial cell wall and cell membranes occurs mainly through electrostatic interactions between the positively charged nanoparticles and negatively charged bacterial surfaces.<sup>172</sup> This results in strong adsorption of the nanoparticles on the bacterial surface resulting in membrane depolarization, which subsequently affects the transport activity of ions, nutrients and essential macromolecules across the membrane.<sup>173</sup> Numerous electron-dense pits and perforations are formed on the membrane surface at the regions of nanoparticle interaction or attachment, especially in case of Ag



NPs and Al<sub>2</sub>O<sub>3</sub> NPs, which clearly demonstrates the damage caused by these nanoparticles to the membrane surface.<sup>174–176</sup> Extensive depolarization of membranes ultimately leads to loss of membrane integrity and disintegration. This results in the leakage of cellular contents like proteins, reducing sugars, nutrients and even ATP from the membrane-compromised cells, rendering the cells inactive. Significant changes in bacterial morphology in terms of shrinkage of the cytoplasm and membrane detachment have been observed upon interaction with Ag NPs, which finally lead to rupture of the cell wall.<sup>175</sup> It is to be noted that the differences in structure, composition and thickness of membranes among Gram-positive and Gram-negative bacteria also contribute towards the differential antibacterial activity observed among the nanoparticles. Ag NPs show greater antibacterial activity towards Gram-negative bacteria,<sup>177</sup> whereas ZnO NPs were found to be more effective against Gram-positive bacteria.<sup>178</sup> The lipopolysaccharide (LPS) present in the outer membrane of Gram-negative bacteria acts as a binding site for the majority of nanoparticles like Ag NP, Cu NP, TiO<sub>2</sub> NP, *etc.*, whereas the teichoic acids and high negative charge of the peptidoglycan layer in Gram-positive bacteria serve as the sites of interaction with nanoparticles.<sup>179</sup> In addition to these, nanoparticles can also directly interact with the carboxyl, sulfhydryl and carbonyl groups of different membrane proteins that span the membranes of both Gram-positive and Gram-negative bacteria, thereby causing further damage to membrane structure and integrity through disruption of these membrane proteins and severely affecting membrane transport of ions and molecules across the membranes. In addition, Ag NPs can negatively regulate the uptake and release of phosphate and potassium ions from bacterial cells.<sup>173</sup>

**4.1.2. Release of toxic ions, cell penetration and destructive interactions with cellular components.** Apart from nanoparticles acting as a whole in exerting their antibacterial action, dissolution or leaching out of ions from metal and metal oxide nanoparticles in aqueous solutions may also act as highly potent and toxic antibacterial agents.<sup>180</sup> These metal ions easily diffuse across the cell membranes and penetrate the bacterial cells, where they exert serious detrimental effects on intracellular structures and macromolecules, leading to bacterial growth inhibition and death. The toxic ions directly interact with functional groups like mercapto (–SH), amino (–NH), and carboxyl (–COOH) groups present on different proteins and enzymes, and also with phosphate groups and nitrogenous bases of nucleic acids. These interactions cause structural alterations which lead to blockage of active sites, loss of function and degradation of the biomacromolecules,<sup>181</sup> thus affecting the normal physiological processes of the cells and ultimately inhibiting the microorganism. Silver ions (Ag<sup>+</sup>) released from Ag NPs have been found to play a very important role in sculpting the highly efficient antibacterial action of Ag NPs.<sup>180</sup> Ag<sup>+</sup> ions bind with the thiol groups of several membrane proteins causing deactivation of proteins involved in transmembrane ATP generation and solute transport across the membrane.<sup>182</sup> Condensation of nucleic acids resulting in

inhibition of replication is also induced by these metal ions. Ag<sup>+</sup> ions have been found to exhibit preferential interaction with the nucleosides of DNA molecules, forming DNA–metal ion complexes, which has serious implications for replication, transcription and cell division.<sup>182</sup> The intercalation of Ag<sup>+</sup> ions between the nitrogenous base pairs results in disruption of H-bonds between the DNA strands, thereby damaging the double helical structure of DNA.<sup>183</sup> Furthermore, conversion of the relaxed form of DNA to the condensed form has also been observed to occur as a result of Ag NPs.<sup>184</sup> Similarly, Cu<sup>2+</sup> ions leaching out of Cu NPs were observed to be the main mediators of DNA damage and degradation.<sup>185</sup>

In addition to metal ions, the nanoparticles themselves can also penetrate the cell by overcoming the membrane barrier. This generally occurs because of the membrane damage caused by the nanoparticles which results in the formation of pores in the membrane, through which the nanoparticles enter the cells. Inside the cells, the nanoparticles along with their ionic counterparts carry out structural and functional damage to the bacterial cells through oxidative and non-oxidative mechanisms. Inactivation of the phosphomannose isomerase enzyme by direct interaction with Ag NPs has also been observed in bacteria, which caused inhibition of sugar metabolism.<sup>186</sup> Similarly, denaturation of DNA and mutation of key DNA repair genes (mutY, mutS, mutM, mutT and nth) have been observed to take place in bacteria *via* direct interactions between Ag NPs and DNA molecules.<sup>187</sup> Ag NPs, due to their ability to penetrate the cells, directly interact with respiratory dehydrogenases involved in the bacterial electron transport system and cause their inhibition or inactivation,<sup>188</sup> thus thwarting the bacterial respiration process. Additionally, Ag NPs inhibit protein synthesis *via* direct interaction with ribosomes and cause its denaturation.<sup>183,189,190</sup> However, not all nanoparticles need to enter the cells to exert their antibacterial action. For example, MgO NPs were found to exhibit excellent antibacterial activities through membrane damage without entering the cells.<sup>191</sup>

**4.1.3. Oxidative stress.** Killing of bacterial cells through the generation of oxidative stress in the form of reactive oxygen species (ROS) or free radicals is a very prominent mechanism of antibacterial action exhibited by the majority of metal and metal oxide nanoparticles.<sup>192</sup> Nanoparticles react with molecular oxygen (O<sub>2</sub>) present in the surrounding air or environment and reduce it to produce different types of ROS, mainly superoxide anion (O<sub>2</sub><sup>–</sup>), hydroxyl radical (OH<sup>•</sup>), hydrogen peroxide (H<sub>2</sub>O<sub>2</sub>) and singlet oxygen species (<sup>1</sup>O<sub>2</sub>).<sup>192</sup> Different nanoparticles show different ROS-producing abilities depending on their structure, density of defect sites and oxygen vacancies. Accumulation of metal nanoparticles along with their toxic ions inside the cells increases the cellular oxidative stress level in bacteria,<sup>193</sup> which leads to subsequent oxidative damage to cellular components like lipids, proteins and nucleic acids. Even at the membrane surface, when nanoparticles are in contact with the bacterial cells, ROS can be generated by these nanoparticles causing direct damage to cell membrane integrity and stability through peroxidation of the

membrane phospholipids. Ag,<sup>194</sup> Cu<sup>185</sup> and ZnO<sup>195</sup> NPs have been found to cause lipid peroxidation in cells through the generation of excessive oxidative stress. Lipid peroxidation is a key mechanism of oxidative membrane damage in bacteria which results in a decrease in membrane fluidity, an increase in membrane permeability and damage/denaturation of other membrane-bound proteins.<sup>196</sup> Oxidation of polyunsaturated lipids results in the generation of peroxide radicals which then act upon other membrane-bound proteins and cause their oxidative inactivation.<sup>197</sup> This extracellular ROS can also diffuse into the cells and participate in further enhancing the intracellular oxidative stress level in bacteria. Oxidative damage to intracellular proteins as a direct result of nanoparticle-induced ROS production has been clearly observed in both Gram-positive and Gram-negative bacteria upon treatment with a wide variety of nanoparticles. Oxidized proteins are easy targets of several proteases that selectively degrade these proteins upon oxidation, thereby inhibiting cell functions and eventually leading to cell death.<sup>193</sup>

The anti-oxidant glutathione (GSH), which acts as a redox regulator in bacterial cells and protects the cells from oxidative damage by maintaining a pro-oxidant–antioxidant equilibrium, has been found to get oxidized to its disulfide form GSSH, leading to its inactivation.<sup>198</sup> Nanoparticles of silver, copper, ZnO and TiO<sub>2</sub> have been found to cause oxidative damage of intracellular bacterial proteins by depleting the GSH levels in cells.<sup>199,200</sup> The ROS-induced oxidative damage to bacterial cells also includes DNA damage, which severely compromises the genetic machinery of bacterial cells and thus inhibits DNA replication and synthesis.<sup>200</sup> DNA damage through single and double-strand breaks, formation of base-sugar adducts and complexation of DNA with other molecules resulting in inhibition of replication are known to be caused by free radicals such as hydroxyl radicals and singlet oxygen.

Photocatalysis is another mechanism by which a number of metal oxide nanoparticles like ZnO and TiO<sub>2</sub> generate ROS.<sup>201</sup> When these nanoparticles are excited with light of a particular energy that is either equal to or greater than their band gap, electrons get excited from the valence band to the conduction band. This process creates highly reactive intermediates called electron–hole pairs, which react with oxygen and water to generate ROS and attack cells and cause damage. In addition to metal oxide nanoparticles, carbon dots have also been shown to exhibit excellent antibacterial activities through the process of photocatalytic ROS production.<sup>202</sup> Upon excitation with light ranging from UV to near-IR, C-dots have been found to generate ROS such as singlet oxygen and hydroxyl radicals which act as the main mediators for their observed antibacterial action.

**4.1.4. Modulation of gene expression and signal transduction pathways.** Bacterial growth, metabolism, replication, nutrient transport, response to stress and several other aspects of survival are tightly regulated by a network of signaling pathways. These pathways involve specific signaling molecules, which relay specific signals for a particular biological function or response, that are expressed through the process of upregu-

lation/downregulation of a set of genes. Proteins play a very crucial role in such pathways where they act as the signaling molecules, and phosphorylation/dephosphorylation of key protein molecules determines the fate of that specific signal. Under normal circumstances, these signaling molecules remain in their precursor form in which they are inactive. Phosphorylation of these precursors results in their activation, which subsequently regulates several key metabolic and structural functions of the cell that are essential for cell survival. Dephosphorylation of that protein again brings it back to its inactive form, ready for relaying a second round of information when required. This reversible phosphorylation/dephosphorylation process of the proteins is a key mechanism in the survival and normal functioning of bacterial cells.<sup>203</sup> Thus, inhibition of protein phosphorylation can seriously hamper signal transduction, thereby causing cell death. Exposure of bacterial cells to Ag NPs has been found to result in dephosphorylation of tyrosine residues of some peptides, which adversely affects the signal transduction in bacteria and inhibits their growth.<sup>204</sup> Similarly, other proteins which are involved in DNA synthesis, replication, transcription, metabolism and the cell cycle can also act as targets for different metal nanoparticles or their leached out toxic ions, which might cause their inactivation through dephosphorylation.

In addition to modulation of signaling pathways, nanoparticles also play a role in regulating bacterial gene expression to a large extent. Exposure of bacterial cells to metal and metal oxide nanoparticles such as Ag, TiO<sub>2</sub>, MgO, CeO<sub>2</sub> has been found to cause differential expression of a variety of genes associated with bacterial membrane structure and function, cellular transport, electron transfer and ATP production, DNA replication and repair, metabolism and stress response (oxidative and non-oxidative). Ag NPs<sup>181</sup> and TiO<sub>2</sub> NPs<sup>205</sup>-induced membrane damage and membrane stress were found to upregulate the expression of genes regulating membrane structure (*bolA*) and envelope proteins such as outer membrane proteins (OmpA, OmpC, OmpF), periplasmic oligopeptide binding protein A (OppA), and D-methionine binding lipoprotein (MetQ).<sup>206</sup> Genes regulating electron transfer (*sdhC*) and bacterial respiration (*cydA* and *cydB*) were found to be differentially expressed in bacteria upon treatment with Ag and CeO<sub>2</sub> NPs, indicating the role of these nanoparticles in disrupting the bacterial electron transport system and respiratory chain.<sup>206,207</sup> Upregulation of genes conferring protection against ROS-mediated oxidative stress is one of the key aspects of gene regulation observed in bacteria upon treatment with nanoparticles, which again establishes the strong role of nanoparticle-induced oxidative stress in killing of bacteria. Genes such as *ahpC*, *aphF*, *katE*, *katG*, *oxyR* and *sod* genes (*A*, *B*, *C*), associated with regulating redox reactions and peroxide metabolism, were differentially regulated in bacteria by Ag and TiO<sub>2</sub> NPs.<sup>205,206</sup> Similarly, Ag and TiO<sub>2</sub> NPs also regulate the expression of genes related to DNA replication, synthesis, and repair. Downregulation of genes like *dnaX*, *holB*, *guaC*, *pyrC*, *gyrA* that are involved in DNA replication and synthesis has been observed in bacterial cells upon treatment with TiO<sub>2</sub>

NPs.<sup>205</sup> Along with this, upregulation of genes involved with DNA repair such as *recN*, *uvrA*, *uvrD*, *umuD*, *ybfE*, *yebG*, *ssb*, *sbmc*, and *nfo* also takes place as a result of treatment with Ag and TiO<sub>2</sub> NPs, thereby showing that the cell upon nanoparticle treatment is subjected to stress that prevents the cell from synthesizing new DNA and also prepares it to repair its damaged DNA for survival.<sup>205,206</sup> Nanoparticles can also regulate different metabolic pathways in bacteria by acting on target proteins. MgO, CuO and TiO<sub>2</sub> nanoparticles have been found to modulate pathways related to metabolism of sugar, nitrogen, amino acids *etc.* through differential regulation of a variety of genes that either upregulated or downregulated a set of proteins essential for cell survival and growth.<sup>191,205,206</sup>

Thus, nanoparticles exert their antibacterial action by directly interacting with the bacterial cell wall and membrane where direct physical contact-mediated as well as ROS-mediated pathways cause damage and disruption of membrane permeability and integrity. This results in leakage of cellular components like sugars, proteins and ATP from the membrane-compromised cells, rendering the cells metabolically inactive. Toxic ions leaching out from nanoparticles further contribute towards the ongoing antibacterial action through direct interaction with cellular proteins, nucleic acids and membranes, causing their denaturation and disintegration. Furthermore, excessive generation of intracellular oxidative stress upon cellular penetration of nanoparticles and their toxic ions leads to oxidative damage to cellular structures and components, which completely disrupts the functional integ-

rity of cells through differential regulation of metabolism and different signal transduction pathways (Fig. 6).

#### 4.2 Mechanism of antiviral action of 0D nanoparticles

As discussed previously, each step in the process of viral infection is a potential target for antiviral agents to act upon for inhibiting viral infection, either by directly inactivating the virus through physical or chemical damage, or by preventing the virus from entering the host cells. These are the two key steps by which majority of nanoparticles (Ag, Au, CuO, SiO<sub>2</sub>, C-dots) act to exert their antiviral action. Ag NPs have been found to inhibit HIV-1 infection by preventing the binding of HIV-1 virus's surface protein gp120 with its receptor CD4 on host cells.<sup>208</sup> This was found to occur because of direct interaction of Ag NPs with the gp120 protein on the virus surface, leading to its structural and functional modification. This inhibited HIV-1 virus infection at the very early stage of virus binding and fusion, thus reducing the infectivity of the virus. In addition to this, the Ag NPs were also found to inhibit HIV-1 infection in both cell-free and cell-associated systems, showing the virucidal property of these nanoparticles to cause direct inactivation of viruses.<sup>208</sup> CuO-NPs have been observed to interfere with attachment and entry of hepatitis C virus (HCV) infectious virions in hepatic host cells.<sup>209</sup> Carbon dots (C-dots) have also been found to exert antiviral activity against a wide variety of viruses by inhibiting the first step of virus-host cell interaction. Inhibition of binding of norovirus virus-like particle (VLP) to histo-blood group antigen (HBGA) recep-

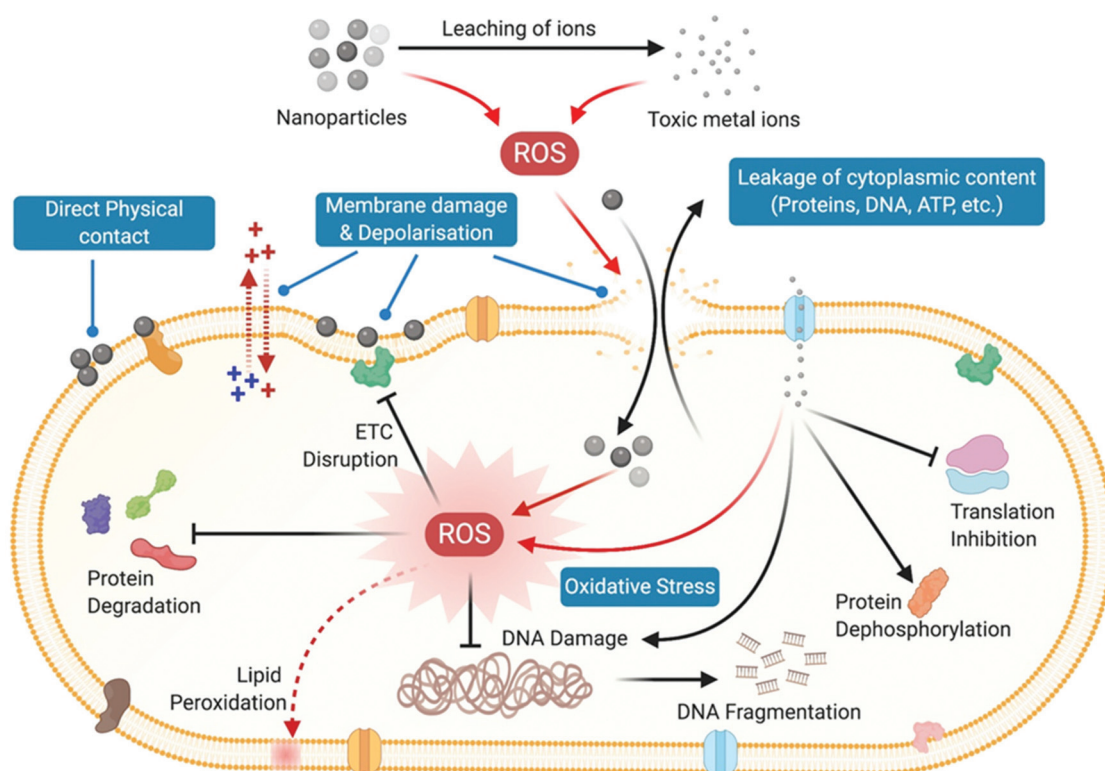


Fig. 6 Schematic showing the mechanism of antibacterial action of 0D nanoparticles.



tors on human cells<sup>210</sup> and blocking of infection by flaviviruses (Japanese encephalitis, Zika, and dengue viruses) and non-enveloped viruses (porcine parvovirus and adenovirus-associated virus)<sup>211</sup> have been found to take place upon treatment of these viruses with C-dots. A recent study has demonstrated that carbon quantum dots (CQDs) can block the Receptor Binding Domain (RBD) of the SARS-CoV-2 spike protein by increasing the extent of the interaction through formation of hydrogen bonds between functional groups on the C-dot surface and spike amino acid residues.<sup>212</sup> In a recent study, molecular docking revealed the anti-viral effect of iron oxides NPs (IONPs) against SARS-CoV-2. It was observed that the strong binding affinity of IONPs to the S1-RBD of viral spike glycoprotein could induce conformational changes in the spike, resulting in virus instability.<sup>213</sup> Nanoparticle coatings made of Ag, CuO and ZnO have been reported to exhibit potent anti-SARS-CoV-2 activity. It has been anticipated that these nanoparticles exhibit antiviral property against SARS-CoV-2 through the release of Ag<sup>+</sup>, Cu<sup>2+</sup> and Zn<sup>2+</sup> ions, which could lyse the membrane by directly adsorbing on the viral envelope and ROS generation.<sup>214</sup> Titanium dioxide (TiO<sub>2</sub>) nanoparticles inactivated the influenza virus H3N2 by destroying the virus envelope, which resulted in the destruction and disintegration of the virions entirely.<sup>215</sup>

The antiviral action can also be exerted at later stages of the viral infection cycle when the viruses have already infected the cells. In such cases, inhibition of viral DNA/RNA replication, damage to the viral genome and induction of a pro-inflammatory phenotype in host cells are the major ways of preventing further infection and killing the virus. Some nanoparticles like Ag, ZnO, CuO, C-dots and Ag<sub>2</sub>S nanoclusters have been found to act at this stage.<sup>216,217</sup> Ag<sub>2</sub>S nanoclusters prevented porcine epidemic diarrhea virus (PEDV) infection in host cells by inhibiting the synthesis of viral negative-strand RNA and also activated the production of IFN-stimulating genes (ISGs) and the expression of proinflammatory cytokines by the host cells, which resulted in generating an anti-viral innate immune response in the host cells, helping to inhibit the PEDV infection.<sup>218</sup> In addition to preventing viral attachment and binding to the host cell, C-dots also exert antiviral action by activating the type-I interferon response in host cells.<sup>219</sup>

Lastly, preventing the virions from budding off the host cell surface is another mechanism through which the viral infection can also be restricted. Ag<sub>2</sub>S nanoclusters were found to inhibit the process of budding off of PEDV virions from Vero cells.<sup>218</sup> The nanoparticles might be able to inhibit the cleavage of hemagglutinin-sialic acid receptor interaction between the virions and the host cell membrane by directly binding to neuraminidase proteins and thereby inactivating it in the process.<sup>220</sup> Hence, inhibiting the virus from entering the host cells seems to be the most common pathway followed by nanoparticles in implementing their antiviral action (Fig. 7).

### 4.3 Mechanism of antibacterial action of 1-D nanotubes

**4.3.1. CNT-bacteria interaction.** The first step in the process of CNTs' antibacterial action is the establishment of

direct physical contact between bacteria and CNTs. This usually takes place through formation of CNT-bacteria aggregates when in suspension (Fig. 8A);<sup>221</sup> however, for nanostructured bactericidal surfaces having CNT pillars or arrays, the physical contact is in the form of adsorption of the bacterial cells on the tips of the vertically aligned CNT structures (Fig. 8B).<sup>222</sup> The length of the nanotubes plays a very crucial role in this initial step of direct contact formation.<sup>223</sup> Smaller nanotubes tend to aggregate among themselves in solution without involving a sufficient number of bacterial cells, thereby reducing the chances of direct physical contact between the nanotubes and bacteria. Longer nanotubes form aggregates with bacterial cells more effectively through a "length-dependent wrapping" mechanism by involving a greater number of bacteria in the aggregate formation process. This improves the effectiveness of the interaction between the two and thus enhances its antibacterial potential.<sup>223,224</sup> In the case of CNT pillars and nanoarrays with high aspect ratio and flexibility, CNTs of shorter length are found to exert more pronounced antibacterial action as compared with longer CNTs due to the difference in their elastic properties.<sup>222</sup> The amount of elastic energy that can be stored in a CNT of shorter length is greater as compared with that of longer CNTs for same horizontal deflection. This process of direct contact sets into motion the subsequent sequence of events leading to membrane damage and oxidative stress.

**4.3.2 Membrane stress.** Once the nanotubes are in contact with the bacterial surface, or more specifically with its outer membrane, the physico-chemical properties of the nanotubes along with their typical tube-like morphology start to exert stress on the bacterial membrane. This event can occur through two pathways:

(i) *Direct puncturing or piercing of the bacterial membrane:* the tubular morphology of the nanotubes makes them behave as "nano-darts" in solution that are capable of directly penetrating through the bacterial lipid bilayer, resulting in loss of membrane permeability and membrane disruption.<sup>221,222</sup> This is mainly due to the "non-specific toxicity" of the CNT arising from its hydrophobicity, which allows it to penetrate or partition itself into the hydrophobic lipid bilayer very efficiently, consequently causing membrane stress.<sup>226</sup> However, in the case of nanostructured bactericidal surfaces with flexible and high aspect ratio nanotube arrays, the process of generation of membrane stress and its subsequent disruption is governed by the flexibility and elasticity of the vertically aligned nanotubes.<sup>222</sup> Owing to this flexible nature, these high aspect ratio nanotubes store a significant amount of elastic energy within them. Upon contact with a bacterial cell, these flexible nanotubes undergo a process of sequential bending and retraction, which subjects the attached cells to progressive stretching and tearing of their adsorbed membranes, ultimately leading to complete membrane deformation and rupture (Fig. 8B).<sup>222</sup> The elastic energy previously stored in these nanostructures is released during this process of sequential bending and retraction of the nanotubes, which acts as the main driving force for inducing the membrane stress. The diameter of nanotubes



Fig. 7 Schematic showing the mechanism of antiviral action of 0D nanoparticles.

plays a very crucial role at this stage in determining the toxicity of the nanotubes towards bacteria.<sup>227</sup> SWCNTs with smaller diameter exert more toxicity through a “diameter-dependent piercing” mechanism in comparison with MWCNTs having a larger diameter.<sup>224,227</sup> The presence of a larger surface area in SWCNTs contributes towards more contact and interaction with the bacterial outer membrane, leading to more membrane perturbation and stress. As a result of this induced membrane stress, a number of genes like Sigma factors  $\sigma^S$  and  $\sigma^E$ , high-pressure stress-related genes, Tol/Pal and PhoPQ two-component system genes associated with maintaining and preserving the integrity of bacterial outer membrane and envelope get up-regulated.<sup>227</sup>

(ii) *Oxidative stress induced membrane damage*: CNTs upon stimulation with light can produce ROS like singlet oxygen species, superoxide anions and hydroxyl radicals, which can directly act upon the bacterial membrane and cause lipid peroxidation that induces conformational changes in membrane proteins, and alters membrane fluidity and integrity, thereby leading to membrane damage and loss in permeability (Fig. 8C).<sup>225</sup> This is mainly due to the “specific or reactive toxicity” of the CNT that arises from its electrophilicity and results in the generation of oxidative stress through the disruption/oxidation of key cellular components like lipids, proteins and nucleic acids.<sup>226</sup> The electronic structure of the nanotubes

determines their reactive nature, with metallic CNTs showing more reactive (oxidative) toxicity towards bacteria as compared with semiconductor CNTs (Fig. 8E).<sup>226</sup> Experiments with anti-oxidant-functionalized CNTs and bare CNTs in the absence of light stimulation have shown inhibition of the antibacterial activity of the CNTs (Fig. 8D). This confirms the pivotal role of ROS-dependent oxidative stress in causing membrane damage, and also establishes that direct physical contact-dependent membrane damage might not be the only process through which the nanotubes exert their antibacterial action.<sup>225</sup>

**4.3.3 Cellular oxidative stress.** The contribution of the “specific or reactive toxicity” of the CNTs towards the overall antibacterial action becomes more prominent and significant once the bacterial membrane integrity is compromised, and it extends towards exerting more detrimental effects on the intracellular machinery of the bacterial cells. Oxidation of intracellular components like glutathione, a thiol-containing peptide which acts as an antioxidant, can take place,<sup>226</sup> thereby disrupting the antioxidant mechanism of the cells and promoting further oxidative damage to the cells through oxidation of nucleic acids and other key proteins essential for cell survival. This process of oxidative damage of the cytoplasmic components of the bacterial cells can take place either by the ROS generated by the nanotubes,<sup>225,227</sup> or can occur in a ROS-independent manner where the membrane-penetrating nano-

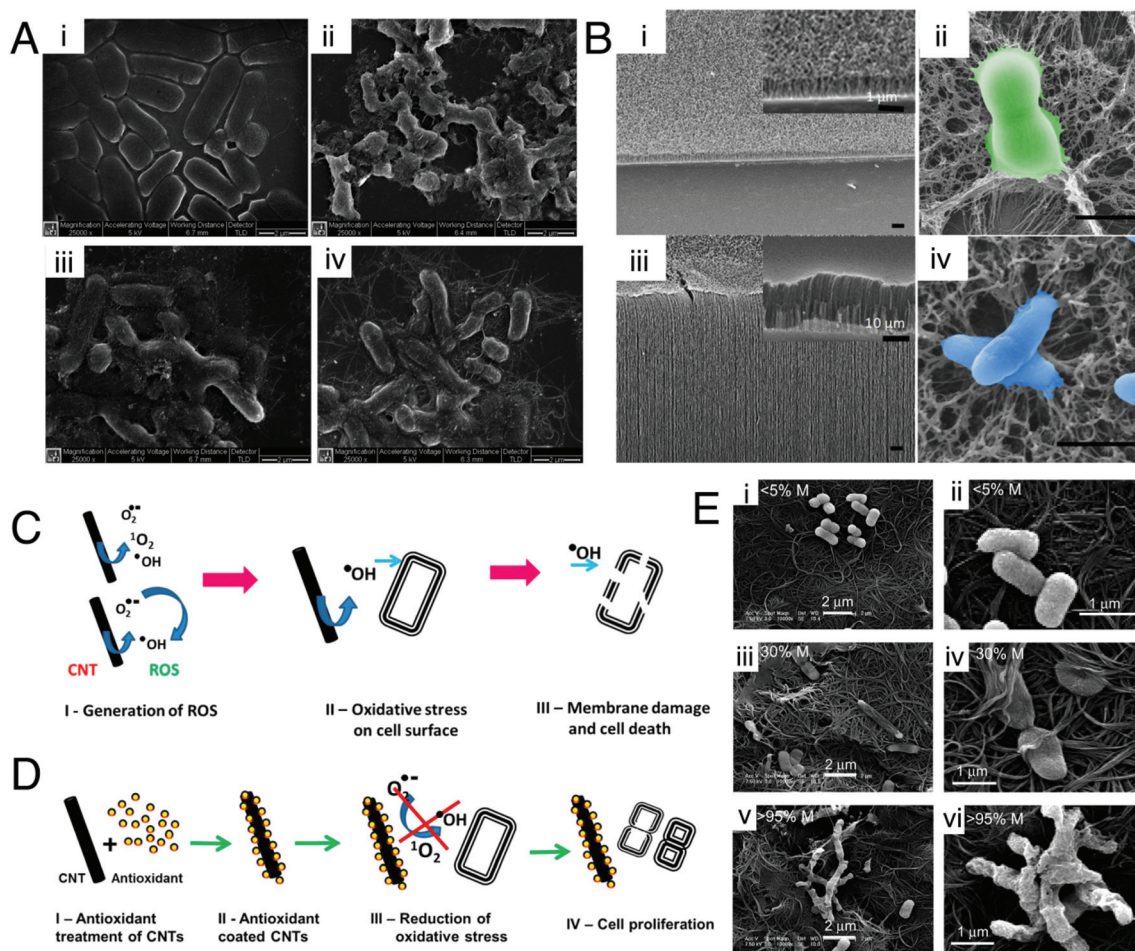


**Fig. 8** Mechanism of antibacterial action of 1-D nanotubes. (A) SEM images of *Salmonella* cells (i) without SWCNTs, and the aggregates of cells and SWCNTs of (ii)  $<1\ \mu\text{m}$ , (iii)  $1\text{--}5\ \mu\text{m}$ , and (iv)  $\sim 5\ \mu\text{m}$ . Reproduced with permission.<sup>221</sup> Copyright 2007, American Chemical Society. (B) SEM images contrasting the heights of the high aspect ratio nanotubes (i)  $1\ \mu\text{m}$  and (ii)  $30\ \mu\text{m}$  VACNTs. False color SEM images of (iii) *S. aureus* and (iv) *P. aeruginosa* attached onto VACNT surfaces, revealing the bending of the CNTs and deformation of the bacterial cell membrane. Reproduced with permission.<sup>222</sup> Copyright 2018, American Chemical Society. (C) Oxidative stress (ROS)-mediated bacterial cell death. Reproduced with permission.<sup>225</sup> Copyright 2014, American Chemical Society. (D) Protection of bacterial cells against oxidative stress by an antioxidant. Reproduced with permission.<sup>225</sup> Copyright 2014, American Chemical Society. (E) Representative SEM images of *E. coli* deposited on SWNT filters. *E. coli* were deposited on the SWNT filter, incubated for 45 min in isotonic saline, and fixed with glutaraldehyde and osmium tetroxide prior to SEM imaging: (i and ii)  $<5\%$  metallic, (iii and iv)  $30\%$  metallic, and (v and vi)  $>95\%$  metallic. Note the differences in cell membrane hydration, structure, and roughness between the three samples. Reproduced with permission.<sup>226</sup> Copyright 2010, American Chemical Society.

tubes can directly oxidize the proteins and nucleic acids through electron transfer.<sup>226</sup> This property is again governed by the electronic structure of the nanotubes, and metallic nanotubes are found to exert more oxidative stress as compared with semiconductor ones.<sup>226</sup> At the molecular level, several genes that are part of bacterial oxidative stress response systems such as *soxRS* and *oxyR* systems are expressed in bacteria as a result of CNT-induced oxidative stress.<sup>227</sup>

**4.3.4 Leakage of cytoplasmic contents.** The apparent physical disruption of the lipid bilayer through puncturing and lipid peroxidation results in leakage of cytoplasmic components like proteins, nucleic acids *etc.* from the compromised bacterial cells.<sup>224,225,227</sup> The membrane stress generated on the bacterial cells by the nanotubes results in the cells losing their physical integrity and morphology, which is coupled with the

detrimental effects of the oxidative stress that disrupts or inhibits key biochemical and metabolic pathways/components of the cells. The combined actions of membrane stress and oxidative stress renders the bacterial cells metabolically inactive, which ultimately leads to cell death.

There are no significant reports demonstrating the antiviral activity of pristine nanotubes. On the contrary, reports suggest that SWCNTs significantly increase the infectivity of influenza H1N1 virus towards lung epithelial cells by inhibiting expression of anti-viral molecules and pro-inflammatory cytokines by the epithelial cells, increasing the expression of viral attachment receptors and through impairment of mitochondrial function.<sup>228,229</sup> Thus, a targeted impairment of anti-viral signaling networks that are vital to immune defense mechanisms in lung cells was induced by the nanotubes.



#### 4.4 Mechanism of antibacterial action of 2-D nanosheets

**4.4.1 Direct physical contact.** The antibacterial activity of nanosheets stems from their direct physical interaction with bacterial cells, more specifically with the bacterial membrane. This is the first and the most crucial step in initiating the process of nanosheet interaction with bacteria and its subsequent events that ultimately lead to cell death. Several factors, like nanosheet size, thickness, degree of oxidation, surface charge, hydrophilicity/hydrophobicity, dispersibility and orientation come into play and influence the nature of this interaction between the nanosheets and bacterial cells.<sup>230</sup> Predominantly influenced by the lateral size of nanosheets and their specific orientation (free floating in suspension or fixed at a particular angle on a substrate) in the interacting environment, the nature or mode of interaction between the nanosheets and bacteria can take place mainly through two mechanisms, namely *surface-area mediated physical interaction*<sup>231,232</sup> and *edge-mediated physical interaction* (Fig. 9A).<sup>233,234</sup> Both these mechanisms of interaction can take place as independent modes/pathways of establishing direct

physical contact with the bacterial membrane or can occur in a sequential manner, the ultimate outcome of which is to exert a membrane-directed physical stress on the bacterial cells in contact.

Sheets having a larger size tend to interact with the bacterial membrane through *surface-area mediated physical interaction*, using their basal planes to come into contact with the membrane surface and tend to arrange themselves flat on the membrane surface.<sup>235</sup> Such kind of interaction generally leads to the “wrapping/trapping” of the cells by the larger-sized sheets (micron sized), which can efficiently wrap around the entire cells and trap them in an isolated environment.<sup>231,235,236</sup> In such events, membrane stress in the form of membrane damage or disruption is not that evident in the bacterial cells; however, studies have shown that it can lead to the formation of patches of upturned phospholipids at the sites of nanosheet attachment, thereby causing membrane perturbations in place of disruptions.<sup>237,238</sup> As shown in studies with GO nanosheets in suspension, bacterial cells were completely wrapped by the nanosheets having larger lateral dimensions, resulting in bac-

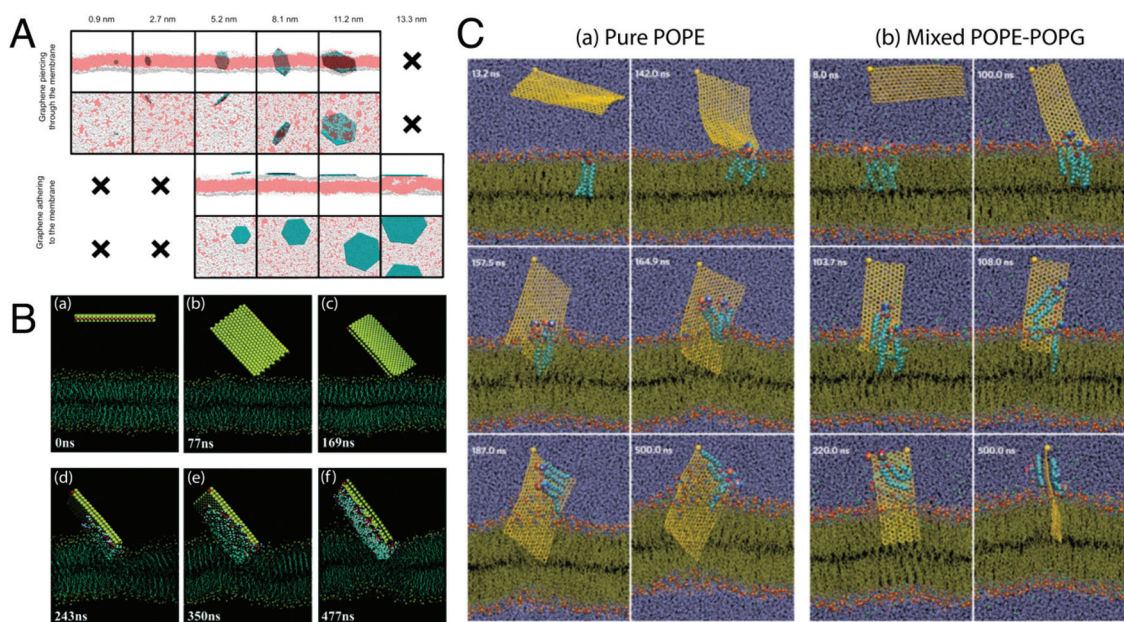


**Fig. 9** Mechanism of antibacterial action of 2-D nanosheets. (A) Illustrative snapshots, at the end of the simulations, of six graphene nanosheets of increasing size. From left to right, sizes of 0.9, 2.7, 5.2, 8.1, 11.2, and 13.3 nm. White: hydrophilic heads of the phospholipids; red: hydrophobic phospholipid tails; petroleum blue: graphenes. For clarity, water is not shown. The top two rows are different perspectives of the six sheets, as are the bottom two rows. Only the five smaller sheets pierce through the membrane. The four larger sheets adhere to the membrane. Situations not observed in the simulations are indicated by “x”. Reproduced with permission.<sup>238</sup> Copyright 2015, American Chemical Society. (B) Representative simulated trajectory of the restrictive simulation. (snapshot time is shown in the lower left corner of each picture.) The MoS<sub>2</sub> nanosheet is shown as a yellow rectangular sandwich structure with S atoms in yellow and Mo atoms in pink. The fixed S atom in the corner of the nanosheet is denoted in red. The phospholipids are represented in blue lines with P atoms as khaki spheres. Extracted phospholipid atoms (within 5 Å of the MoS<sub>2</sub> nanosheet) are shown as coloured spheres (oxygen, red; nitrogen, navy blue; hydrogen, white; carbon, aqua; and phosphorus, khaki). The molecules of the physiological saline solution are omitted here for expediently displaying the phenomenon of phospholipid extraction. Reproduced with permission.<sup>234</sup> Copyright 2018, Royal Society of Chemistry. (C) Graphene nanosheet insertion and lipid extraction. (a and b) Representative simulated trajectories of graphene nanosheet insertion and lipid extraction in the outer membrane (pure POPE) and inner membrane (3 : 1 mixed POPE–POPG) of *E. coli* (the snapshot times are shown in the top left corners). Water is shown in violet and the phospholipids in tan lines with hydrophilic charged atoms as coloured spheres (hydrogen, white; oxygen, red; nitrogen, dark blue; carbon, cyan; phosphorus, orange). The graphene sheet is shown as a yellow-bonded sheet with a large sphere marked at one corner as the restrained atom in simulations. Extracted phospholipids are shown as larger spheres. Reproduced with permission.<sup>240</sup> Copyright 2013, Nature Nanotechnology.

terial inactivation.<sup>235</sup> This observed inactivation actually occurred through the inhibition of proliferation of cells trapped within the sheets. As a result of trapping by the nanosheets the bacterial cells were isolated from their surrounding environment, which prevented the passage and entry of nutrients into the cells. However, such a process of bacterial inactivation through the wrapping/trapping pathway was found to be reversible in nature, as the trapped bacterial cells upon sonication could come out from the traps and regain their viability, and thus this process does not lead to complete bacterial inactivation.<sup>236</sup> On the other hand, sheets with smaller size possess sharp edges and corners, which make them behave as “nano-knives” and as a result interact with the bacterial membranes through an *edge-mediated physical interaction* process that involves direct puncturing or piercing of the lipid bilayer, leading to penetration of the nanosheets into the cytoplasmic region of the cells by creating pores in the bacterial membrane.<sup>238</sup> Such an interaction is also observed with nanosheets that have been arranged in the form of a coating or placed on a substrate in a specific orientation.<sup>233</sup>

The orientation of the nanosheets plays a key role in determining their mode of interaction with the bacterial membrane. Smaller sheets are found to mostly interact with the membrane through a perpendicular orientation, allowing them to penetrate more efficiently through the membrane using their edges, as evidenced in molecular dynamics (MD) simulation studies.<sup>238</sup> However, the antibacterial efficiency of nanosheets is not always dictated by a perpendicular orientation. Tilted nanosheets arranged at a particular angle on a substrate are also found to be extremely potent in displaying antibacterial activity.<sup>239</sup> This emphasizes the importance of availability of sharp edges and their density in achieving strong antibacterial action. The vertical alignment of the nanosheets on a substrate<sup>233</sup> or their tilted arrangement in a particular orientation<sup>239</sup> results in providing a surface with a high density of sharp edges, which interact with bacterial cells through the *edge-mediated physical interaction* process.

**4.4.2 Membrane stress.** Be it surface area-mediated physical interaction or edge-mediated, the attachment/adsorption of the nanosheets on the membrane surface and its subsequent penetration results in creating a membrane stress on the bacterial cells.<sup>232</sup> This process of generation of membrane stress by nanosheets has been investigated in great detail using both experimental and theoretical approaches, which have deciphered the key events taking place at the membrane surface of the bacterial cells as a result of these interactions. The results from all these studies involving different kinds of nanosheets ranging from graphene-based materials like GO and rGO,<sup>241</sup> transition metal dichalcogenides such as MoS<sub>2</sub>,<sup>242–244</sup> WS<sub>2</sub>,<sup>243,245,246</sup> MoSe<sub>2</sub>,<sup>243</sup> to MXenes<sup>247</sup> and black phosphorous<sup>248</sup> nanosheets, provide a picture of this membrane damage process which seems to be quite uniform and shared among these different classes of nanosheets, thereby helping us in proposing a general mechanism of membrane-directed antibacterial action of these nanosheets by taking into consideration the “nanosheets” as a family.

Upon establishment of primary physical contact with the phospholipid bilayer, the nanosheets begin to interact with the lipid head groups of the membrane through a wide variety of interactive forces such as electrostatic, van der Waals's and hydrophobic interactions, depending on the chemical nature of the nanosheets. Graphene sheets interact primarily through hydrophobic interactions,<sup>240</sup> while the oxygen-containing functional groups of GO and rGO,<sup>238</sup> and Mo and S atoms of MoS<sub>2</sub> nanosheets<sup>234</sup> interact through electrostatic forces with the phospholipid heads (Fig. 9B & C). As a result, the nanosheets start to embed themselves into the phospholipid membranes, creating dents or troughs on the membrane surface.<sup>234</sup> These membrane perturbations lead to the generation of patches of upturned phospholipids on the surface, as discussed before, and mark the initiation of membrane disruption.<sup>237,238</sup> The embedding of the nanosheets into the lipid bilayer intensifies the ongoing interactions between the lipid molecules and the nanosheet surface, as a result of which deepening of dents is observed which in turn exposes the hydrophobic lipid tails buried in the membrane core. Strong interactions take place between the nanosheet surface and the hydrophobic lipid tails resulting in destructive extraction of phospholipid molecules from the membrane onto the surface of the nanosheets. MD simulation studies using both graphene<sup>240</sup> and MoS<sub>2</sub><sup>234</sup> nanosheets clearly show the process of phospholipid extraction by these nanosheets. MoS<sub>2</sub> nanosheets were found to mediate this process through the formation of dents on the membrane surface (Fig. 9B), whereas graphene nanosheets caused direct penetration of the lipid bilayer along with lipid extraction (Fig. 9C). This event of phospholipid extraction disturbs the membrane integrity to a large extent, causing rapid depolarization of the membranes.<sup>244</sup> The membranes lose their permeability barrier and become more vulnerable to further damage. However, it is to be noted that at this stage, the membrane is still intact and not fully disintegrated. For complete disintegration of the membrane to take place, the already embedded nanosheets now need to further penetrate into the membrane and puncture through the lipid bilayer. At this point, the edge-mediated physical interaction starts to dominate. The process of phospholipid extraction weakens the bilayer structure, as a result of which it becomes easier for the embedded nanosheets to penetrate further into the membrane, ultimately causing the membrane to rupture and disintegrate. This results in leakage of the cytoplasmic contents of the cells, such as DNA, RNA and proteins.

**4.4.3 Disruption of bacterial respiration and metabolic inactivation.** The membrane-directed antibacterial action of nanosheets discussed in the previous section has been found to directly affect bacterial respiration through the inactivation of the biological function of the inner membrane-bound respiratory dehydrogenase enzymes (proteins) that are an integral part of the bacterial respiratory chain. Biological activity of membrane-bound enzymes greatly depends on their proper orientation and on their association with the membrane. Physical disruption of the lipid bilayer by nanosheets can cause possible detachment of these proteins from the mem-

brane surfaces, causing them to lose their structural integrity and thus function. This inhibition of respiratory dehydrogenases in turn uncouples bacterial respiration from the oxidative phosphorylation pathway, consequently causing metabolic inactivation and arrest. Studies with MoS<sub>2</sub> nanosheets have shown the ability of these nanosheets to cause inhibition of lactate dehydrogenase (LDH) activity in bacterial cells, followed by metabolic inactivation and loss in cell viability.<sup>244</sup> This shows that the physical damage caused by the nanosheets to the bacterial cells has direct detrimental effects on key intracellular biochemical and metabolic pathways of the cells, which also contributes towards the observed antibacterial action of these nanosheets.

**4.4.4 Oxidative stress.** The size of nanosheets has been found to play a significant role in determining their antibacterial activity. Several studies have been carried out in this direction to understand how the lateral size of nanosheets influences their antibacterial activity.<sup>231,235,244,247</sup> However, the results from different studies have provided a contradictory picture, with some studies showing larger-sized nanosheets to be more antibacterial in nature, and others establishing smaller-sized ones to be more efficient in killing bacteria. Thus, a clear and general view on the mechanism of antibacterial action of nanosheets based solely on their lateral size cannot be presented. This necessitates looking for other factors that might also play a definitive role in sculpting the antibacterial action of nanosheets. One such factor is the oxidation capacity of nanosheets. Nanosheets have been shown to induce oxidative stress in bacterial cells as another prominent mode of action to exert their antibacterial activity.<sup>241,242,244,246,247</sup> Detailed investigations into understanding the nanosheet-mediated oxidative stress-induced bacterial cell death have revealed that these sheet-like nanostructures are capable of generating oxidative stress through both ROS-dependent as well as ROS-independent pathways.

- *ROS-dependent oxidative stress:* Nanosheets are capable of generating ROS or free radicals by interacting with molecular oxygen available in the surrounding environment. The oxygen molecules adsorb on the defects and edges of the nanosheets and get reduced into free radicals such as superoxide anion, hydrogen peroxide, singlet oxygen and hydroxyl radical.<sup>231,249</sup> The degree of oxidation and the presence of surface defects on the nanosheets are key factors in determining the ROS-producing abilities of nanosheets. Studies on GO and rGO have shown GO sheets to exert more antibacterial activity as compared with rGO, through generation of more intracellular ROS.<sup>250,251</sup> The greater oxidation capacity of GO nanosheets can be attributed to the presence of numerous oxygen-containing functional groups and increased defect density on their surface in comparison with rGO.<sup>251–253</sup> In addition to these factors, the size of nanosheets also influences their oxidation capacity and thus antibacterial action. In studies involving GO,<sup>231</sup> MoS<sub>2</sub><sup>244</sup> and MXene<sup>247</sup> nanosheets, a size-dependent antibacterial action was observed to take place, with smaller nanosheets showing stronger antibacterial action as compared

with their larger counterparts. This is again due to the higher oxidative nature of smaller nanosheets because with decrease in size, the density of surface defects increases, and the higher the defect density, the greater is the ROS-generating ability of the nanosheets. The membrane-directed antibacterial action of nanosheets also results in the formation of oxidative stress inside the bacterial cells. This, coupled with the nanosheets' intrinsic material property to generate abiotic ROS, overpowers the bacterial antioxidant mechanism and results in disturbing the redox equilibrium of the cells through GSH oxidation. The free radicals cause further damage to the cells through oxidation of key bacterial components like DNA, RNA, proteins, lipids *etc.*, thereby rendering them non-functional.<sup>254</sup> Along with these, the oxidative stress generated can also damage the bacterial membrane through peroxidation of the membrane phospholipids, which in turn generates more reactive oxygen species like lipid peroxide radicals that participate in propagating the on-going oxidative damage.<sup>255</sup>

- *Charge (electron) transfer mediated ROS-independent oxidative stress:* Apart from ROS-mediated oxidative stress, nanosheets can also exert oxidative stress on bacteria through a mechanism arising from the conductive nature of nanosheets without the involvement of free radical generation. Studies with GO,<sup>233</sup> MoS<sub>2</sub>,<sup>242,243,256</sup> WS<sub>2</sub>,<sup>243</sup> and MoSe<sub>2</sub><sup>243</sup> nanosheets, which are all known to have good electrical conductivity, have shown their involvement in directly disrupting or inhibiting a key biochemical process or structure of bacterial cells through the process of electron transfer. The nanosheets, upon interacting with the bacterial membrane, form a conductive layer on the surface of the membrane. This conductive layer then behaves as an electron pump and transfers electrons from bacterial membrane or from intracellular components to the outside environment, thereby oxidizing the bacterial components in the process.<sup>241,257</sup> Several studies have reported the direct GSH oxidizing properties of different nanosheets, which have helped in establishing the fact that nanosheets are also capable of directly disturbing the redox equilibrium of bacterial cells and create oxidative stress in a ROS-independent manner. The higher GSH oxidizing property of rGO observed in comparison with GO sheets is also attributed to the better conductivity of rGO than GO.<sup>241</sup> Such a process of nanosheet-assisted electron transfer from bacteria is widely considered to be the primary mechanism of antibacterial action of nanosheets, especially when such nanosheets are employed in the form of coatings and substrates.

The above discussions provide a clear picture that the antibacterial action of nanosheets is not just a result of physical damage to the bacterial cells caused by the sharp edges/corners of these nanosheets, but also due to the chemical nature of the different nanosheets that gives rise to their oxidative mode of action. The consequences of membrane-directed mechano-bactericidal action of nanosheets coupled with ROS-dependent and independent pathways of oxidative stress generation make the bacterial cells completely lose their structural and functional integrity, finally leading to cell death (Fig. 10).



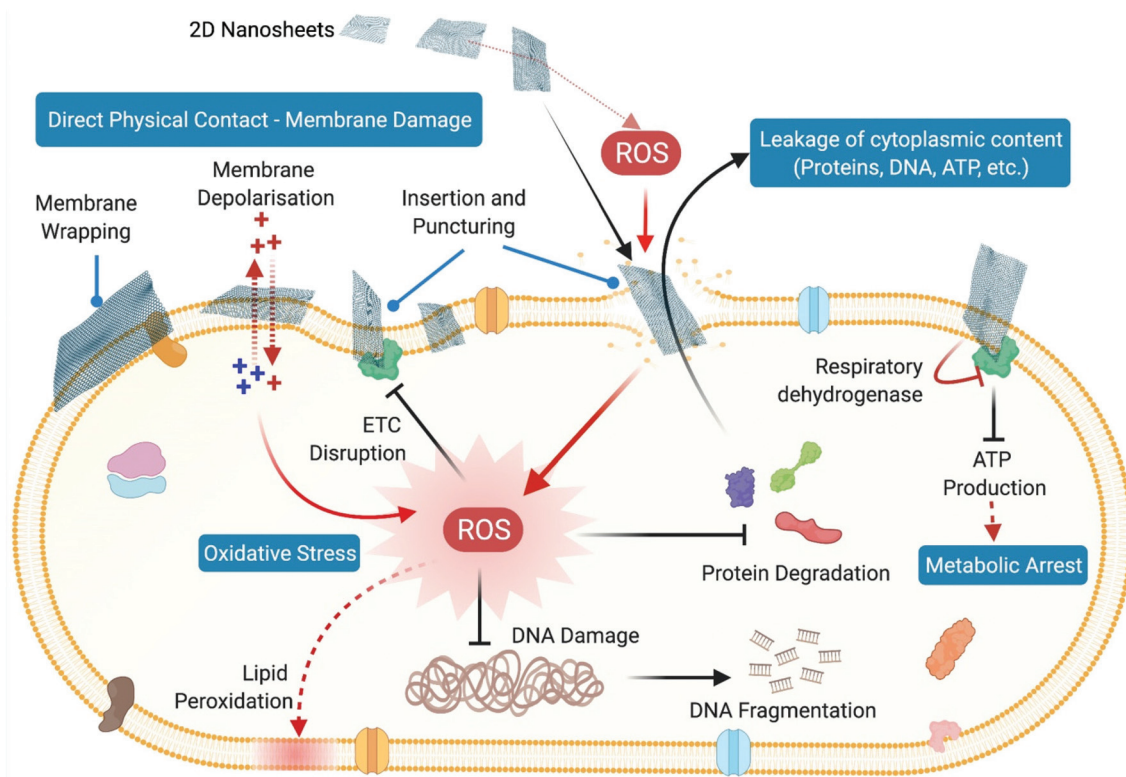


Fig. 10 Schematic showing the mechanism of antibacterial action of 2D nanosheets.

#### 4.5 Mechanism of antiviral action of 2D nanosheets

The antiviral action of nanosheets has been attributed to their negative surface charge and the presence of a layered nanoscale morphology with sharp edges and corners.<sup>258</sup> The primary mechanism of antiviral action observed in studies involving GO and rGO nanosheets against both enveloped and non-enveloped viruses is the direct interaction of the nanosheets with the virus surface through strong electrostatic interactions, which ultimately results in inducing physical damage to the viral structure through a sharp edge-mediated effect, as also observed in case of bacteria.<sup>258</sup>

The importance of a monolayer structure of nanosheets in determining their antiviral activity was evaluated by comparing the antiviral properties of graphite, graphite oxide, graphene oxide and reduced graphene oxide,<sup>258</sup> and it was observed that only GO and rGO with a monolayer structure and nanoscale size could demonstrate significant antiviral activity, whereas graphite and graphite oxide, which act as precursors to these nanostructures, showed very weak or complete absence of antiviral activity due to their multi-layered morphology and larger lateral size.<sup>258</sup>

In addition to morphology and size, surface charge is another key factor influencing the antiviral action of nanosheets. Studies indicated that it is the charge density and not charge identity that actually determines the antiviral activity of these nanosheets.<sup>259</sup> GO and rGO both possess similar net negative charge but differ in the type of functional

groups present on their surfaces. The antiviral activity of GO and rGO was found to be similar, demonstrating that the presence of different functional groups did not affect the antiviral action.<sup>258</sup> This has been further supported by comparing the antiviral properties of GO and sulfonated rGO nanosheets.<sup>259</sup> It was observed that the introduction of additional negatively charged sulfonate groups in the GO structure did not improve its antiviral activity, as both GO and sulfonated rGO had the same negative charge density.

Detailed studies on understanding the exact nature of viral inactivation by GO and MoS<sub>2</sub> nanosheets have shown that these nanosheets are not able to inhibit viral infection in cell lines if the virus has already attached to the cells or the cells have been pre-incubated with nanosheets before virus addition.<sup>258,260</sup> The nanosheets were found to be effective only when they were pre-incubated with the virus particles prior to infection. Thus, the main mode of action of these nanosheets is by preventing the entry of viruses into cells by capturing them prior to cellular attachment.<sup>258,259</sup>

Once the nanosheets get attached to the surface of the virus particles, the presence of sharp edges and corners of nanosheets can cause physical damage to the virus structure as evidenced through transmission electron microscopy in the case of both enveloped and non-enveloped viruses. It has been observed that GO nanosheets are quite capable of completely disrupting the virus morphology by damaging the viral envelope, capsid, and viral proteins such as spike proteins which are present on the surface of the virus. Interaction of GO

nanosheets with pseudorabies virus (PRV) and PEDV was found to destroy the viral envelope and spike proteins of these viruses<sup>258</sup> (Fig. 11A–D). Similar results were also observed with enterovirus 71 (EV71) whose regular hexahedron morphology was completely broken by GO, and with influenza A virus subtype H9N2 where the spherical/filamentous virus particles were found to be collapsed upon interaction with GO nanosheets and their spike proteins were drastically destroyed<sup>261</sup> (Fig. 11E). Similarly, physical disruption of herpes simplex virus-1 (HSV-1) by MoS<sub>2</sub> nanosheets has also been observed. The sharp edges of the nanosheets were found to disrupt the viral envelope, leading to leakage of internal viral material.<sup>260</sup>

This disruption of the viral structure and viral proteins by nanosheets can also arise from the chemical properties of nanosheets, where the nanosheets can mediate their antiviral action through disruption of key protein–protein interactions that play crucial roles in maintaining virus structural integrity

and infectivity. MD simulation showed that graphene nanosheets can interact very strongly with Ebola virus VP40 oligomers through hydrophobic interactions and break apart these oligomers by penetrating through them (Fig. 11F). VP40 proteins are very crucial in forming the Ebola virus matrix.<sup>262</sup> VP40 hexamers undergo oligomerization through their C-terminal domains with adjacent hexamers, forming VP40 filaments which make up the entire Ebola virus matrix. Thus, disrupting the formation of these filaments can directly inactivate the virus and act as a mode of antiviral action. Graphene sheets, owing to their strong hydrophobic nature, insert themselves through the hydrophobic CTD–CTD interactions of the hexamers and separate the hexameric domains from each other. Similar observations have also been reported for HIV-1 integrase proteins, where the dimeric conformation of the integrase protein is destroyed by graphene nanosheets<sup>263</sup> (Fig. 11G).

From molecular docking analyses it has been recently revealed that GO binds with strong affinity to the SARS-CoV-2

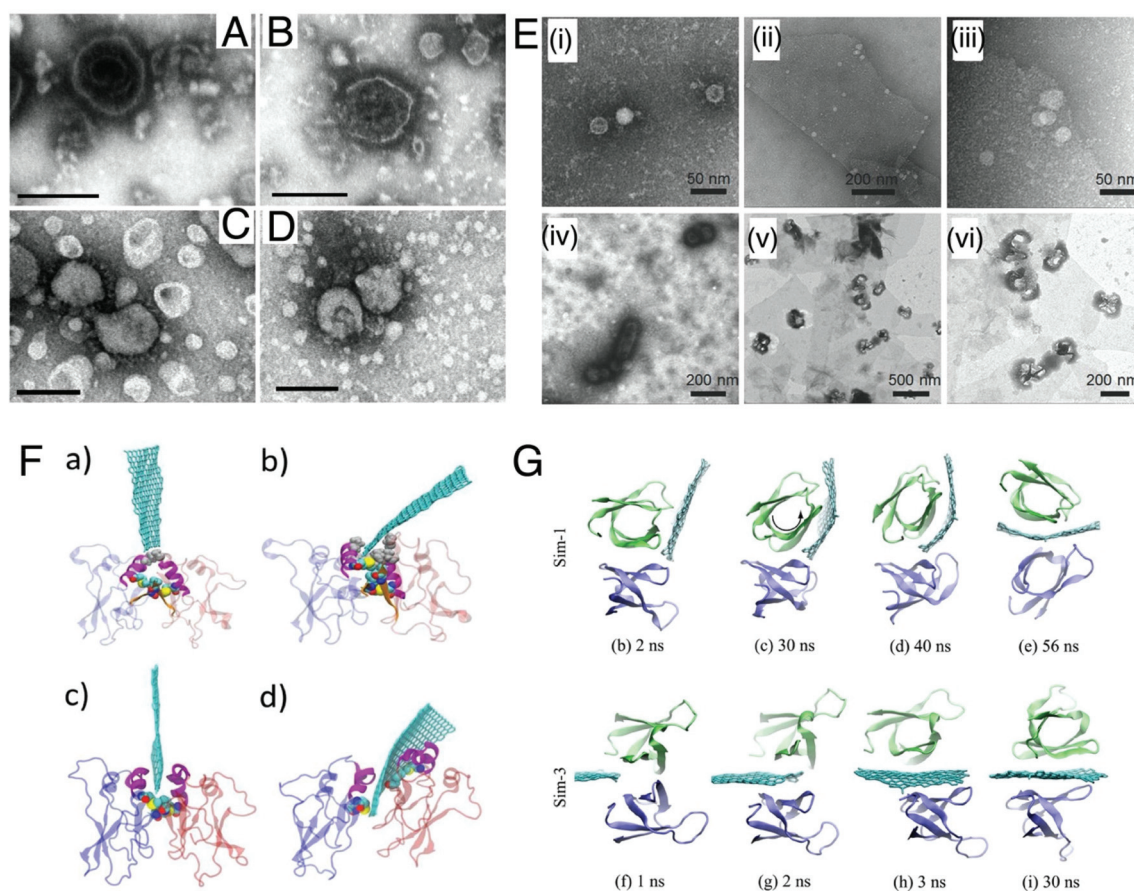


**Fig. 11** Mechanism of antiviral action of 2D nanosheets. Transmission electron microscopic images of GO-treated viruses. (A) PRV control; (B) PRV treated with GO for 1 h; (C) PEDV control; and (D) PEDV incubated with GO for 1 h. Scale bars: 200 nm (A and B) and 100 nm (C and D). Reproduced with permission.<sup>258</sup> Copyright 2015, American Chemical Society. (E) TEM images of negative stained native EV71 (i) and GO captured EV71 complexes at (ii) low and (iii) high magnification; TEM images of negative stained (iv) H9N2 and GO captured H9N2 complexes at (v) low and (vi) high magnification with thermal heating treatment. Reproduced with permission.<sup>261</sup> Copyright 2015, Wiley. (F) MD snapshots of the graphene insertion through the hexamer CTD–CTD interface. (a and b) Initial breaking of A229/P234 and (c and d) graphene disrupting the M241–I307 pair and inserting farther into the interface. Reproduced with permission.<sup>262</sup> Copyright 2017, Elsevier. (G) Snapshots of the insertion process of a graphene sheet into the dimer. Reproduced with permission.<sup>263</sup> Copyright 2015, American Chemical Society.

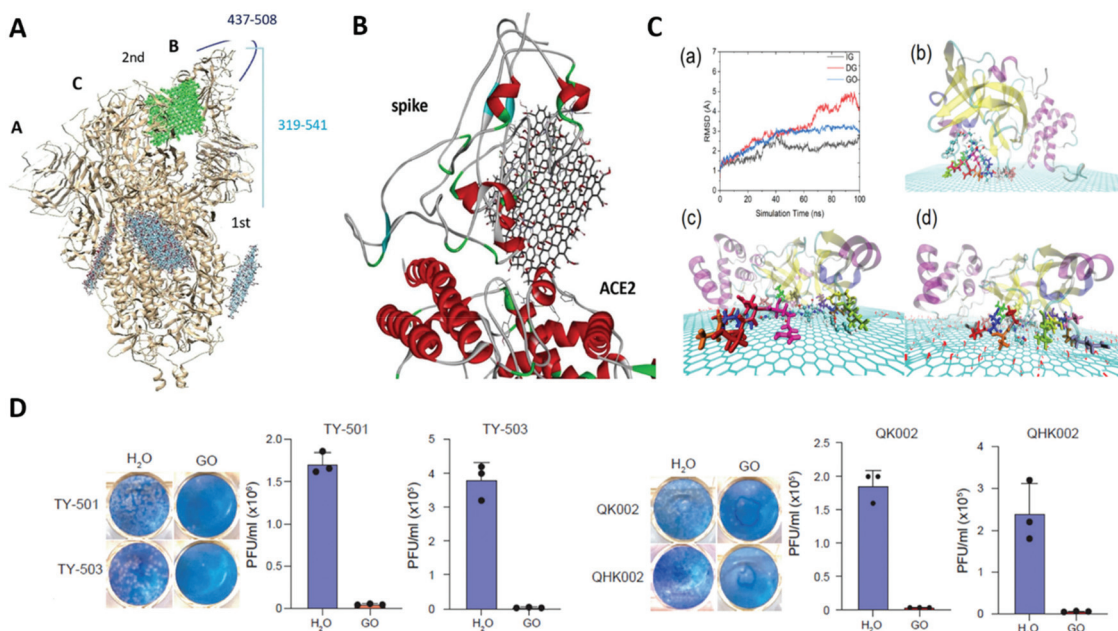


**Fig. 12** Anti-SARS-CoV-2 activity of 2D nanosheets. (A) Binding of GO at different sites of open state of spike protein (6VYB). (B) Binding of GO with spike-ACE2 complex (6M0J) with binding affinity  $-9.1 \text{ kcal mol}^{-1}$ . Reproduced with permission. Copyright 2021, Wiley.<sup>264</sup> (C) Deactivation of the SARS-CoV-2 protease M<sup>Pro</sup> by GO. (a) RMSD of the active pocket of M<sup>Pro</sup> for all systems during 100 ns MD simulations. Representative snapshots of M<sup>Pro</sup> adsorbed onto (b) IG, (c) DG, and (d) GO. Reproduced with permission.<sup>265</sup> Copyright 2021, American Chemical Society. (D) Anti-SARS-CoV-2 activity against Brazilian strains (TY7-501 and TY7-503) and U.K. strains (QK002 and QHN001) in the presence and absence of GO ( $100 \mu\text{g mL}^{-1}$ ) using plaque assay. Reproduced with permission.<sup>267</sup> Copyright 2021, American Chemical Society.

spike glycoprotein and its mutated form (Fig. 12A & B).<sup>264</sup> The GO nanosheets were also capable of interacting with the host receptor ACE2 and its complex with the spike protein spike-ACE2 complex. Upon binding, GO nanosheets acted as a hydrogen donor and acceptor at major positions on the surface of the spike protein and interacted with the proteins *via* non-covalent interactions. Among such interactions, GO interaction at the RBD region of SARS-CoV-2 *via* electrostatic and hydrogen bonding is of great significance for being an antiviral agent.<sup>264</sup> Another study provided detailed insight about deactivation of the SARS-CoV-2 protease M<sup>Pro</sup> by disabling of the active site and reduced expression upon direct interaction with graphene materials (pristine graphene, GO and defective graphene) (Fig. 12C).<sup>265</sup> Molecular dynamics simulations showed that M<sup>Pro</sup> adsorbs onto the surface of graphene through hydrophobic interaction, while with its derivatives the protein interacted with its hydrophilic amino acids. The molecular structure of M<sup>Pro</sup> and its active site is stabilized by several hydrogen bonds. The effective adsorption of the active site on graphene derivative caused hydrogen bond breakage, which induced instability in the posture and conformation of the active site resulting in loss of function (viral replication and transcription) of M<sup>Pro</sup>. By damaging the active site of M<sup>Pro</sup>, graphene has emerged as an efficient inhibitor of SARS-CoV-2 infection.<sup>265</sup> In another recent study, Shahbazi *et al.* studied the effect of multiple 2D nanomaterials (bismuthene, graphene, phosphorene, P-doped graphene, and functionalized P-doped graphene) on SARS-CoV-2 and claimed

that the surface chemistry and architecture of these nanomaterials has a strong influence on the inhibition of SARS-CoV-2 infectivity. Nearly all 2D nanomaterials reduced the hydrophobic interaction and hydrogen bonding between spike and ACE2 by distorting the stable conformation of the spike structure. Along with this, the graphene and functionalized P-doped graphene nanosheets directly contacted with lipid, hydrophobic components, and ion channels of the envelope membrane of the virion and penetrated inside the membrane, causing viral membrane disruption. Inactivation of M<sup>Pro</sup> by functionalized P-doped graphene nanosheet makes it significant inhibitor to combat SARS-CoV-2 infection completely.<sup>266</sup> GO has proven to be an excellent adsorbent nanomaterial due to the availability of negatively charged oxygen functional groups on its dual sides. The positive patches of amino acid residues present on the spike glycoprotein and nucleocapsid protein of SARS-CoV-2 subsequently adsorb *via* electrostatic interaction onto the negative surface of GO nanosheet. This direct contact of GO-viral protein causes destruction of structural integrity of both viral proteins, thereby leading to loss of function followed by viral deactivation. The presence of the oxygen functional group plays significant role in exhibiting antiviral activity against the SARS-CoV-2 as compared with reduced GO nanosheets due to its ability to facilitate effective electrostatic interaction with virions (Fig. 12D).<sup>267</sup> Bidimensional graphene nanosheets are flexible in nature too, which along with polyglycerol sulfate (PGS) and aliphatic chain functionalization provides a plat-



form for containment of the Feline coronavirus (FCoV) *via* electrostatic interactions with alkyl chains of graphene nanosheets and rupturing *via* hydrophobic interactions directly with graphene nanosheets. In the virustatic and virucidal mode of action, the functionalized graphene nanosheets prohibit the entry of virions by exhibiting electrostatic interaction between negatively charged Polyglycerol Sulfate present in graphene derivative and positively charged amino acid residues of the spike glycoprotein of FCoV and inactivation by causing envelope disintegration upon interacting with lipids of the viral envelope.<sup>268</sup> This has led to the utilization of graphene and its derivatives as an antiviral material for developing personal protective equipment such as face masks.<sup>269,270</sup>

Thus, nanosheets with a net negative surface charge and a monolayer morphology exert their antiviral activity by strongly attaching themselves to the surface of positively charged virus particles through electrostatic interactions, thereby capturing them on their surface. This in turn inhibits the attachment of these viruses to the cell surface and thus prevents viral entry into the cells. This is coupled with nanosheet edge-mediated physical destruction of the viruses, which finally leads to their inactivation.

## 5. Conclusion and future perspective

In summary, the mechanism of action of antibacterial and antiviral agents ranging from macroscale polymers, proteins and peptides to nanoscale particles, tubes and sheets is provided. The mechanism of antibacterial action of macroscale biomaterials, such as antimicrobial peptides and polymers, mainly occurs by targeting the bacterial membrane. These biomaterials damage the cell membrane either through “pore-forming” pathways or *via* “non-pore-forming” pathways of membrane disruption ultimately leading to cellular lysis. In addition to membrane-targeting mechanisms, antimicrobial peptides also exert their bactericidal activities by inhibiting any of the key intracellular processes like nucleic acids synthesis, cell wall synthesis, protein synthesis and so on. Polymers, both natural and synthetic, can have intrinsic antimicrobial activities, or they can be functionalized with different chemical groups to mimic the antimicrobial peptides. Polymers exert their antimicrobial activity mainly by targeting the cell membrane through pathways similar to that of antimicrobial peptides. Peptido-polysaccharides, which are a combination of peptides and polysaccharides, act as bacterial cell wall mimics and thus interfere with cell wall synthesis and induce osmotic instability.

The antibacterial action of nanoparticles, nanotubes and nanosheets is mainly dictated by two main pathways: (i) membrane damage, and (ii) oxidative stress. All kinds of nanostructures, irrespective of their size, morphology and surface chemistry, initiate the process of antibacterial activity by establishing direct physical contact with the bacterial membrane; this then proceeds towards the induction of membrane stress followed by membrane damage. This process of generation of

membrane stress differs among the different classes of nanostructures. Nanoparticles mostly adhere to the membrane surface and cause local perturbations leading to changes in membrane permeability and integrity, without directly penetrating or puncturing the lipid bilayer. On the other hand, nanotubes and nanosheets directly puncture and pierce the bacterial membranes using their sharp edges, corners and narrow tips, creating pores in the lipid bilayer. The generation of oxidative stress in the form of ROS is observed for all types of nanostructures, and leads to oxidative damage of lipids, proteins, nucleic acids and membrane components. Nanoparticles are found to exert this oxidative stress mainly through a ROS-dependent pathway, whereas nanotubes and nanosheets contribute to the overall oxidative stress-mediated cell death involving both ROS-dependent and ROS-independent pathways. The intrinsic material properties of nanotubes and nanosheets participate in direct electron transfer to intracellular components such as proteins and nucleic acids, leading to their oxidation without the involvement of free radicals. On the other hand, cellular uptake of nanoparticles and their dissolved/leached out ions delivers direct damage to proteins and nucleic acids through dephosphorylation, intercalation, condensation and disintegration.

Focusing on the virucidal properties of biomaterials, it can be stated that polymers and peptides act by making each step of the viral infection and replication a potential target. However, nanoparticles can exert their antiviral action at multiple stages of virus infection, such as directly damaging the viral structure, preventing the virus from entering the host cells by binding to receptors, inhibition of viral DNA/RNA replication, damage to the viral genome, induction of a pro-inflammatory phenotype in host cells and by blocking the budding off and release of viral progenies from the host cell surface. Nanosheets are found to act upon the viruses by directly destroying their structure and membrane/envelope proteins. Nanotubes, on the other hand, are not found to exert antiviral activity.

Overall, this review provides a comprehensive understanding about how different classes of biomaterials interact with bacteria and viruses to exert their antimicrobial action. It is very important to understand the nature and specific outcome of such interactions to develop better antimicrobial biomaterials. By knowing the detailed mechanism of action of the biomaterials, researchers will be able to develop novel antimicrobial agents against which bacteria or viruses cannot easily become resistant. Furthermore, understanding these diverse mechanisms will enable researchers to choose the most appropriate biomaterials for specific applications, such as for biofilm eradication, development of coating materials for biomedical implants, wound healing materials, tissue engineering scaffolds *etc.* It will also assist in developing better strategies for designing next-generation antimicrobial PPEs and antiviral agents. Combining macroscale and nanoscale biomaterials into a single antimicrobial platform may provide biomaterials with better therapeutic efficacy through the combined effects of the individual properties of each component.



## Conflicts of interest

The authors declare no competing financial interests.

## Acknowledgements

The authors acknowledge the support from the BioX Centre and Advanced Materials Research Centre (AMRC), the Indian Institute of Technology Mandi for Research and Infrastructure facility. Shounak Roy would like to acknowledge DST INSPIRE Fellowship [IF160513] for providing doctoral fellowship. Fig. 1–4, 6, 7 and 10 and the graphical abstract was created with BioRender.com and the authors gratefully acknowledge BioRender.

## References

- M. L. Cohen, *Nature*, 2000, **406**, 762–767.
- D. E. Bloom and D. Cadarette, *Front. Immunol.*, 2019, **10**, 549.
- H. H. Khachfe, M. Chahrour, J. Sammouri, H. Salhab, B. E. Makki and M. Fares, *Cureus*, 2020, **12**(3), e7313.
- A. Findlater and I. I. Bogoch, *Trends Parasitol.*, 2018, **34**, 772–783.
- J. P. Koplan, T. C. Bond, M. H. Merson, K. S. Reddy, M. H. Rodriguez, N. K. Sewankambo and J. N. Wasserheit, *Lancet*, 2009, **373**, 1993–1995.
- N. I. Nii-Trebi, *BioMed Res. Int.*, 2017, **2017**, 5245021.
- W. Hall, *Superbugs: An arms race against bacteria*, Harvard University Press, 2018.
- B. Aslam, W. Wang, M. I. Arshad, M. Khurshid, S. Muzammil, M. H. Rasool, M. A. Nisar, R. F. Alvi, M. A. Aslam and M. U. Qamar, *Infect. Drug Resist.*, 2018, **11**, 1645.
- M. Frieri, K. Kumar and A. Boutin, *J. Infect. Public Health*, 2017, **10**, 369–378.
- I. Yelin and R. Kishony, *Cell*, 2018, **172**, 1136–1136.
- H.-P. Shih, X. Zhang and A. M. Aronov, *Nat. Rev. Drug Discovery*, 2018, **17**, 19–33.
- L.-j. Zhang and R. L. Gallo, *Curr. Biol.*, 2016, **26**, R14–R19.
- S. Y. Tan and Y. Tatsumura, *Singapore Med. J.*, 2015, **56**, 366.
- T. Franklin and G. Snow, in *Biochemistry and molecular biology of antimicrobial drug action*, Springer, 1998, pp. 43–59.
- K. Matsuzaki, O. Murase, N. Fujii and K. Miyajima, *Biochemistry*, 1996, **35**, 11361–11368.
- P. Li, C. Zhou, S. Rayatpisheh, K. Ye, Y. F. Poon, P. T. Hammond, H. Duan and M. B. Chan-Park, *Adv. Mater.*, 2012, **24**, 4130–4137.
- N. Baig, I. Kammakam and W. Falath, *Mater. Adv.*, 2021, **2**, 1821–1871.
- E. O. Ogunsona, R. Muthuraj, E. Ojogbo, O. Valerio and T. H. Mekonnen, *Appl. Mater. Today*, 2020, **18**, 100473.
- G. G. Luo and S. J. Gao, *J. Med. Virol.*, 2020, **92**, 399.
- C. S. Adamson, K. Chibale, R. J. Goss, M. Jaspars, D. J. Newman and R. A. Dorrington, *Chem. Soc. Rev.*, 2021, **50**, 3647–3655.
- M. Ito, M. Baba, A. Sato, R. Pauwels, E. De Clercq and S. Shigetani, *Antiviral Res.*, 1987, **7**, 361–367.
- A. Grassauer, R. Weinmuellner, C. Meier, A. Pretsch, E. Prieschl-Grassauer and H. Unger, *Virol. J.*, 2008, **5**, 1–13.
- L. Yu, K. Li, J. Zhang, H. Jin, A. Saleem, Q. Song, Q. Jia and P. Li, *ACS Appl. Bio Mater.*, 2022, **5**(2), 366–393.
- M. A. Abdalla, *J. Nat. Med.*, 2016, **70**, 708–720.
- W. C. Wimley, *ACS Chem. Biol.*, 2010, **5**, 905–917.
- E. F. Palermo, I. Sovadinova and K. Kuroda, *Biomacromolecules*, 2009, **10**, 3098–3107.
- E. R. Cobo and K. Chadee, *Pathogens*, 2013, **2**, 177–192.
- M. Zasloff, *Lancet*, 2002, **360**, 1116–1117.
- H. Tanabe, T. Sato, J. Watari, A. Maemoto, M. Fujiya, T. Kono, T. Ashida, T. Ayabe and Y. Kohgo, *Helicobacter*, 2008, **13**, 370–379.
- C. Zhou, X. Qi, P. Li, W. N. Chen, L. Mouad, M. W. Chang, S. S. Leong and M. B. Chan-Park, *Biomacromolecules*, 2010, **11**, 60–67.
- J. Gao, M. Wang, F. Wang and J. Du, *Biomacromolecules*, 2016, **17**, 2080–2086.
- J. C. Tiller, C. J. Liao, K. Lewis and A. M. Klivanov, *Proc. Natl. Acad. Sci. U. S. A.*, 2001, **98**, 5981–5985.
- Y. Hu, Y. Du, J. Yang, Y. Tang, J. Li and X. Wang, *Polymer*, 2007, **48**, 3098–3106.
- M. Kong, X. G. Chen, C. S. Liu, C. G. Liu and X. H. Meng, *Colloids Surf., B*, 2008, **65**, 197–202.
- Y. Zhang, J. Jiang and Y. Chen, *Polymer*, 1999, **40**, 6189–6198.
- H. Tan, R. Ma, C. Lin, Z. Liu and T. Tang, *Int. J. Mol. Sci.*, 2013, **14**, 1854–1869.
- Y. Chen, S. Worley, J. Kim, C.-I. Wei, T.-Y. Chen, J. Santiago, J. Williams and G. Sun, *Ind. Eng. Chem. Res.*, 2003, **42**, 280–284.
- T. J. Cuthbert, B. Hisey, T. D. Harrison, J. F. Trant, E. R. Gillies and P. J. Ragogna, *Angew. Chem., Int. Ed.*, 2018, **57**, 12707–12710.
- M. N. Stadtmueller, S. Bhatia, P. Kiran, M. Hilsch, V. Reiter-Scherer, L. Adam, B. Parshad, M. Budt, S. Klenk, K. Sellrie, D. Lauster, P. H. Seeberger, C. P. R. Hackenberger, A. Herrmann, R. Haag and T. Wolff, *J. Med. Chem.*, 2021, **64**, 12774–12789.
- B. P. Mowery, S. E. Lee, D. A. Kissounko, R. F. Epand, R. M. Epand, B. Weisblum, S. S. Stahl and S. H. Gellman, *J. Am. Chem. Soc.*, 2007, **129**, 15474–15476.
- S. Saidjalolov, Z. Edoo, M. Fonvielle, L. Mayer, L. Iannazzo, M. Arthur, M. Etheve-Quellejeu and E. Braud, *Chemistry*, 2021, **27**, 3542–3551.
- H. Gleiter, *Acta Mater.*, 2000, **48**, 1–29.
- V. Pokropivny and V. Skorokhod, *Phys. E*, 2008, **40**, 2521–2525.
- W. Niu, L. Zhang and G. Xu, *Nanoscale*, 2013, **5**, 3172–3181.

- 45 P. Innocenzi and L. Stagi, *Chem. Sci.*, 2020, **11**, 6606–6622.
- 46 H. Sun, L. Wu, W. Wei and X. Qu, *Mater. Today*, 2013, **16**, 433–442.
- 47 A. Al-Jumaili, S. Alancherry, K. Bazaka and M. V. Jacob, *Materials*, 2017, **10**, 1066.
- 48 A. Jaiswal, S. S. Ghosh and A. Chattopadhyay, *Chem. Commun.*, 2012, **48**, 407–409.
- 49 R. Hirlekar, M. Yamagar, H. Garse, M. Vij and V. Kadam, *Asian J. Pharm. Clin. Res.*, 2009, **2**, 17–27.
- 50 T. Mocan, C. T. Matea, T. Pop, O. Mosteanu, A. D. Buzoianu, S. Suciuc, C. Puia, C. Zdrehus, C. Iancu and L. Mocan, *Cell. Mol. Life Sci.*, 2017, **74**, 3467–3479.
- 51 S. Lal, J. H. Hafner, N. J. Halas, S. Link and P. Nordlander, *Acc. Chem. Res.*, 2012, **45**, 1887–1895.
- 52 J. Lu, H. Liu, X. Zhang and C. H. Sow, *Nanoscale*, 2018, **10**, 17456–17476.
- 53 B. Mandl, J. Stangl, E. Hilner, A. A. Zakharov, K. Hillerich, A. W. Dey, L. Samuelson, G. Bauer, K. Deppert and A. Mikkelsen, *Nano Lett.*, 2010, **10**, 4443–4449.
- 54 G. Milano, S. Porro, I. Valov and C. Ricciardi, *Adv. Electron. Mater.*, 2019, **5**, 1800909.
- 55 K. S. Novoselov, A. K. Geim, S. V. Morozov, D. Jiang, Y. Zhang, S. V. Dubonos, I. V. Grigorieva and A. A. Firsov, *Science*, 2004, **306**, 666–669.
- 56 G. R. Bhimanapati, Z. Lin, V. Meunier, Y. Jung, J. Cha, S. Das, D. Xiao, Y. Son, M. S. Strano and V. R. Cooper, *ACS Nano*, 2015, **9**, 11509–11539.
- 57 R. Kurapati, K. Kostarelos, M. Prato and A. Bianco, *Adv. Mater.*, 2016, **28**, 6052–6074.
- 58 C. Tan, X. Cao, X.-J. Wu, Q. He, J. Yang, X. Zhang, J. Chen, W. Zhao, S. Han and G.-H. Nam, *Chem. Rev.*, 2017, **117**, 6225–6331.
- 59 C. Gokce, C. Gurcan, O. Besbinar, M. A. Unal and A. Yilmazer, *Nanoscale*, 2021, **14**, 239–249.
- 60 V. Yadav, S. Roy, P. Singh, Z. Khan and A. Jaiswal, *Small*, 2019, **15**, 1803706.
- 61 K. Matsuzaki, *Adv. Exp. Med. Biol.*, 2019, **1117**, 9–16.
- 62 G. Ehrenstein and H. Lecar, *Q. Rev. Biophys.*, 1977, **10**, 1–34.
- 63 M. S. Sansom, *Prog. Biophys. Mol. Biol.*, 1991, **55**, 139–235.
- 64 K. Matsuzaki, O. Murase, N. Fujii and K. Miyajima, *Biochemistry*, 1996, **35**, 11361–11368.
- 65 S. J. Ludtke, K. He, W. T. Heller, T. A. Harroun, L. Yang and H. W. Huang, *Biochemistry*, 1996, **35**, 13723–13728.
- 66 D. Sengupta, H. Leontiadou, A. E. Mark and S. J. Marrink, *Biochim. Biophys. Acta*, 2008, **1778**, 2308–2317.
- 67 B. Bechinger and K. Lohner, *Biochim. Biophys. Acta*, 2006, **1758**, 1529–1539.
- 68 E. Gazit, I. R. Miller, P. C. Biggin, M. S. Sansom and Y. Shai, *J. Mol. Biol.*, 1996, **258**, 860–870.
- 69 M. Vaara and T. Vaara, *Antimicrob. Agents Chemother.*, 1994, **38**, 2498–2501.
- 70 M. C. Wiener and S. H. White, *Biophys. J.*, 1992, **61**, 434–447.
- 71 A. Wiese, M. Münstermann, T. Gutschmann, B. Lindner, K. Kawahara, U. Zähringer and U. Seydel, *J. Membr. Biol.*, 1998, **162**, 127–138.
- 72 M. Miteva, M. Andersson, A. Karshikoff and G. Otting, *FEBS Lett.*, 1999, **462**, 155–158.
- 73 S. Ludtke, K. He and H. Huang, *Biochemistry*, 1995, **34**, 16764–16769.
- 74 S. L. Grage, S. Afonin, S. Kara, G. Buth and A. S. Ulrich, *Front. Cell Dev. Biol.*, 2016, **4**, 65.
- 75 H. W. Huang, *Biochim. Biophys. Acta, Biomembr.*, 2020, **1862**, 183395.
- 76 L. Jau and H. B. Fung, *Clin. Ther.*, 2004, **26**, 1728–1757.
- 77 E. F. Haney, S. Nathoo, H. J. Vogel and E. J. Prenner, *Chem. Phys. Lipids*, 2010, **163**, 82–93.
- 78 J. P. Powers, A. Tan, A. Ramamoorthy and R. E. Hancock, *Biochemistry*, 2005, **44**, 15504–15513.
- 79 R. M. Epand and R. F. Epand, *J. Pept. Sci.*, 2011, **17**, 298–305.
- 80 G. Pabst, S. L. Grage, S. Danner-Pongratz, W. Jing, A. S. Ulrich, A. Watts, K. Lohner and A. Hickel, *Biophys. J.*, 2008, **95**, 5779–5788.
- 81 H. Brötz, G. Bierbaum, A. Markus, E. Molitor and H. G. Sahl, *Antimicrob. Agents Chemother.*, 1995, **39**, 714–719.
- 82 R. A. Salomón and R. N. Fariás, *J. Bacteriol.*, 1992, **174**, 7428–7435.
- 83 M. Ishikawa, T. Kubo and S. Natori, *Biochem. J.*, 1992, **287**(Pt 2), 573–578.
- 84 C. B. Park, H. S. Kim and S. C. Kim, *Biochem. Biophys. Res. Commun.*, 1998, **244**, 253–257.
- 85 G. A. Birkemo, T. Lüders, Ø. Andersen, I. F. Nes and J. Nissen-Meyer, *Biochim. Biophys. Acta*, 2003, **1646**, 207–215.
- 86 M. Mardirossian, R. Grzela, C. Giglione, T. Meinnel, R. Gennaro, P. Mergaert and M. Scocchi, *Chem. Biol.*, 2014, **21**, 1639–1647.
- 87 A. Patrzykat, C. L. Friedrich, L. Zhang, V. Mendoza and R. E. Hancock, *Antimicrob. Agents Chemother.*, 2002, **46**, 605–614.
- 88 C. L. Friedrich, A. Rozek, A. Patrzykat and R. E. Hancock, *J. Biol. Chem.*, 2001, **276**, 24015–24022.
- 89 M. Dangkulwanich, C. R. H. Raetz and A. H. Williams, *Sci. Rep.*, 2019, **9**, 3947.
- 90 R. H. Bianculli, J. D. Mase and M. D. Schulz, *Macromolecules*, 2020, **53**, 9158–9186.
- 91 S. Sarrazin, W. C. Lamanna and J. D. Esko, *Cold Spring Harbor Perspect. Biol.*, 2011, **3**, a004952.
- 92 V. Cagno, E. D. Tseligka, S. T. Jones and C. Tapparel, *Viruses*, 2019, **11**(7), 596.
- 93 C. Herrscher, P. Roingard and E. Blanchard, *Cells*, 2020, **9**(6), 1486.
- 94 H. Jenssen, J. H. Andersen, D. Mantzilas and T. J. Gutteberg, *Antiviral Res.*, 2004, **64**, 119–126.
- 95 E. M. Jones, A. Smart, G. Bloomberg, L. Burgess and M. R. Millar, *J. Appl. Bacteriol.*, 1994, **77**, 208–214.
- 96 J. H. Andersen, H. Jenssen and T. J. Gutteberg, *Antiviral Res.*, 2003, **58**, 209–215.
- 97 T. Murakami, T. Nakajima, Y. Koyanagi, K. Tachibana, N. Fujii, H. Tamamura, N. Yoshida, M. Waki,

- A. Matsumoto, O. Yoshie, T. Kishimoto, N. Yamamoto and T. Nagasawa, *J. Exp. Med.*, 1997, **186**, 1389–1393.
- 98 H. Tamamura, T. Murakami, M. Masuda, A. Otaka, W. Takada, T. Ibuka, H. Nakashima, M. Waki, A. Matsumoto, N. Yamamoto, *et al.*, *Biochem. Biophys. Res. Commun.*, 1994, **205**, 1729–1735.
- 99 V. C. A. Matanic and V. Castilla, *Int. J. Antimicrob. Agents*, 2004, **23**, 382–389.
- 100 M. Wachinger, A. Kleinschmidt, D. Winder, N. von Pechmann, A. Ludvigsen, M. Neumann, R. Holle, B. Salmons, V. Erfle and R. Brack-Werner, *J. Gen. Virol.*, 1998, **79**, 731–740.
- 101 M. Krepstakies, J. Lucifora, C. H. Nagel, M. B. Zeisel, B. Holstermann, H. Hohenberg, I. Kowalski, T. Gutschmann, T. F. Baumert, K. Brandenburg, J. Hauber and U. Protzer, *J. Infect. Dis.*, 2012, **205**, 1654–1664.
- 102 M. M. Ali, G. A. Karasneh, M. J. Jarding, V. Tiwari and D. Shukla, *J. Virol.*, 2012, **86**, 6434–6443.
- 103 A. V. Domashevskiy and D. J. Goss, *Toxins*, 2015, **7**, 274–298.
- 104 N. Yahi, J. Fantini, K. Mabrouk, C. Tamalet, P. de Micco, J. van Rietschoten, H. Rochat and J. M. Sabatier, *J. Virol.*, 1994, **68**, 5714–5720.
- 105 M. A. Matica, F. L. Aachmann, A. Tøndervik, H. Sletta and V. Ostafe, *Int. J. Mol. Sci.*, 2019, **20**, 5889.
- 106 S. Roy, M. Kumari, P. Haloi, S. Chawla, V. B. Konkimalla, A. Kumar, H. K. Kashyap and A. Jaiswal, *Biomater. Sci.*, 2022, **10**, 581–601.
- 107 T. J. Franklin and G. A. Snow, *Biochemistry and molecular biology of antimicrobial drug action*, Springer Science & Business Media, 2005.
- 108 T. Ikeda, H. Yamaguchi and S. Tazuke, *Antimicrob. Agents Chemother.*, 1984, **26**, 139–144.
- 109 T. Tashiro, *Macromol. Mater. Eng.*, 2001, **286**, 63–87.
- 110 T. Ikeda, H. Hirayama, H. Yamaguchi, S. Tazuke and M. Watanabe, *Antimicrob. Agents Chemother.*, 1986, **30**, 132–136.
- 111 E. R. Kenawy and Y. A. G. Mahmoud, *Macromol. Biosci.*, 2003, **3**, 107–116.
- 112 S. Lenoir, C. Pagnouille, C. Detrembleur, M. Galleni and R. Jérôme, *J. Polym. Sci., Part A: Polym. Chem.*, 2006, **44**, 1214–1224.
- 113 P. H. Sellenet, B. Allison, B. M. Applegate and J. P. Youngblood, *Biomacromolecules*, 2007, **8**, 19–23.
- 114 A. Kanazawa, T. Ikeda and T. Endo, *J. Polym. Sci., Part A: Polym. Chem.*, 1993, **31**, 1441–1447.
- 115 E.-R. Kenawy, S. Worley and R. Broughton, *Biomacromolecules*, 2007, **8**, 1359–1384.
- 116 L. Kou, J. Liang, X. Ren, H. Kocer, S. Worley, Y.-M. Tzou and T. Huang, *Ind. Eng. Chem. Res.*, 2009, **48**, 6521–6526.
- 117 B. Demir, R. M. Broughton, M. Qiao, T.-S. Huang and S. Worley, *Molecules*, 2017, **22**, 1582.
- 118 I. Cerkez, H. B. Kocer, S. Worley, R. Broughton and T. Huang, *Langmuir*, 2011, **27**, 4091–4097.
- 119 H. B. Kocer, *Prog. Org. Coat.*, 2012, **74**, 100–105.
- 120 P. Li, C. Zhou, S. Rayatpisheh, K. Ye, Y. F. Poon, P. T. Hammond, H. Duan and M. B. Chan-Park, *Adv. Mater.*, 2012, **24**, 4130–4137.
- 121 Y. Chen, L. Yu, B. Zhang, W. Feng, M. Xu, L. Gao, N. Liu, Q. Wang, X. Huang, P. Li and W. Huang, *Biomacromolecules*, 2019, **20**, 2230–2240.
- 122 M. J. Carlucci, L. A. Scolaro, M. D. Nosedá, A. S. Cerezo and E. B. Damonte, *Antiviral Res.*, 2004, **64**, 137–141.
- 123 E. B. Damonte, M. C. Matulewicz and A. S. Cerezo, *Curr. Med. Chem.*, 2004, **11**, 2399–2419.
- 124 M. J. Carlucci, M. Ciancia, M. C. Matulewicz, A. S. Cerezo and E. B. Damonte, *Antiviral Res.*, 1999, **43**, 93–102.
- 125 M. J. Carlucci, L. A. Scolaro and E. B. Damonte, *J. Med. Virol.*, 2002, **68**, 92–98.
- 126 R. Davis, S. Zivanovic, D. H. D'Souza and P. M. Davidson, *Food Microbiol.*, 2012, **32**, 57–62.
- 127 X. Su, S. Zivanovic and D. H. D'Souza, *J. Food Prot.*, 2009, **72**, 2623–2628.
- 128 M. Ito, M. Baba, A. Sato, R. Pauwels, E. De Clercq and S. Shigeta, *Antiviral Res.*, 1987, **7**, 361–367.
- 129 M. Baba, R. Pauwels, J. Balzarini, J. Arnout, J. Desmyter and E. De Clercq, *Proc. Natl. Acad. Sci. U. S. A.*, 1988, **85**, 6132–6136.
- 130 H. Mitsuya, D. J. Looney, S. Kuno, R. Ueno, F. Wong-Staal and S. Broder, *Science*, 1988, **240**, 646–649.
- 131 S. Mazumder, P. K. Ghosal, C. A. Pujol, M. J. Carlucci, E. B. Damonte and B. Ray, *Int. J. Biol. Macromol.*, 2002, **31**, 87–95.
- 132 M. A. Sosa, F. Fazely, J. A. Koch, S. V. Vercellotti and R. M. Ruprecht, *Biochem. Biophys. Res. Commun.*, 1991, **174**, 489–496.
- 133 J. Trincherro, N. M. Ponce, O. L. Córdoba, M. L. Flores, S. Pampuro, C. A. Stortz, H. Salomón and G. Turk, *Phytother. Res.*, 2009, **23**, 707–712.
- 134 S. C. Feldman, S. Reynaldi, C. A. Stortz, A. S. Cerezo and E. B. Damonte, *Phytomedicine*, 1999, **6**, 335–340.
- 135 N. M. Ponce, C. A. Pujol, E. B. Damonte, M. L. Flores and C. A. Stortz, *Carbohydr. Res.*, 2003, **338**, 153–165.
- 136 M. Baba, R. Snoeck, R. Pauwels and E. de Clercq, *Antimicrob. Agents Chemother.*, 1988, **32**, 1742–1745.
- 137 A. Grassauer, R. Weinmuellner, C. Meier, A. Pretsch, E. Prieschl-Grassauer and H. Unger, *Virol. J.*, 2008, **5**, 107.
- 138 J. Mercer, M. Schelhaas and A. Helenius, *Annu. Rev. Biochem.*, 2010, **79**, 803–833.
- 139 M. Kim, J. H. Yim, S. Y. Kim, H. S. Kim, W. G. Lee, S. J. Kim, P. S. Kang and C. K. Lee, *Antiviral Res.*, 2012, **93**, 253–259.
- 140 C. B. Buck, C. D. Thompson, J. N. Roberts, M. Müller, D. R. Lowy and J. T. Schiller, *PLoS Pathog.*, 2006, **2**, e69.
- 141 L. B. Talarico and E. B. Damonte, *Virology*, 2007, **363**, 473–485.
- 142 L. B. Talarico, C. A. Pujol, R. G. Zibetti, P. C. Faría, M. D. Nosedá, M. E. Duarte and E. B. Damonte, *Antiviral Res.*, 2005, **66**, 103–110.
- 143 W. Wang, P. Zhang, C. Hao, X. E. Zhang, Z. Q. Cui and H. S. Guan, *Antiviral Res.*, 2011, **92**, 237–246.

- 144 X. Xianliang, G. Meiyu, G. Huashi and L. Zelin, *Chin. J. Mar. Drugs*, 2000, **19**, 15–18.
- 145 K. C. Queiroz, V. P. Medeiros, L. S. Queiroz, L. R. Abreu, H. A. Rocha, C. V. Ferreira, M. B. Jucá, H. Aoyama and E. L. Leite, *Biomed. Pharmacother.*, 2008, **62**, 303–307.
- 146 X. Xianliang, D. Hua, G. Meiyu, L. Pingfang, L. Yingxia and G. Huashi, *Chin. J. Mar. Drugs*, 2000, **19**, 4–8.
- 147 B.-f. Jiang, X.-f. Xu, L. Li and W. Yuan, *Mod. Prev. Med.*, 2003, **30**, 517–518.
- 148 E. V. Turner and G. Sonnenfeld, *Infect. Immun.*, 1979, **25**, 467–469.
- 149 G. Zhou, Y. Sun, H. Xin, Y. Zhang, Z. Li and Z. Xu, *Pharmacol. Res.*, 2004, **50**, 47–53.
- 150 H. Yuan, J. Song, X. Li, N. Li and J. Dai, *Cancer Lett.*, 2006, **243**, 228–234.
- 151 M. Lüscher-Mattli, *Antiviral Chem. Chemother.*, 2000, **11**, 249–259.
- 152 D. Huskens, K. Vermeire, A. T. Profy and D. Schols, *Antiviral Res.*, 2009, **84**, 38–47.
- 153 M. J. Keller, B. Zerhouni-Layachi, N. Cheshenko, M. John, K. Hogarty, A. Kasowitz, C. L. Goldberg, S. Wallenstein, A. T. Profy, M. E. Klotman and B. C. Herold, *J. Infect. Dis.*, 2006, **193**, 27–35.
- 154 R. Rupp, S. L. Rosenthal and L. R. Stanberry, *Int. J. Nanomed.*, 2007, **2**, 561–566.
- 155 C. S. Dezzutti, V. N. James, A. Ramos, S. T. Sullivan, A. Siddig, T. J. Bush, L. A. Grohskopf, L. Paxton, S. Subbarao and C. E. Hart, *Antimicrob. Agents Chemother.*, 2004, **48**, 3834–3844.
- 156 J. Chung, Y. Jung, C. Hong, S. Kim, S. Moon, E. A. Kwak, B. J. Hwang, S. H. Park, B. L. Seong, D. H. Kweon and W. J. Chung, *J. Colloid Interface Sci.*, 2021, **583**, 267–278.
- 157 T. Tanaka, K. Nakashima, S. Tsuji, X. Han, J. Zhao, Y. Honda, K. Sakakibara, Y. Kurebayashi, T. Takahashi and T. Suzuki, *Polym. Chem.*, 2019, **10**, 5124–5130.
- 158 S. Tsuji, Y. Aso, H. Ohara and T. Tanaka, *J. Polym. Sci.*, 2020, **58**, 548–556.
- 159 E. D. Clercq, *Nat. Rev. Drug Discovery*, 2007, **6**, 941–941.
- 160 L. Menéndez-Arias, *Virus Res.*, 2008, **134**, 124–146.
- 161 S. Agrawal, J. Tang and D. Brown, *J. Chromatogr. A*, 1990, **509**, 396–399.
- 162 F. Eckstein, *J. Am. Chem. Soc.*, 1970, **92**, 4718–4723.
- 163 A. Vaillant, *ACS Infect. Dis.*, 2018, **5**, 675–687.
- 164 R. D. Cardin, F. J. Bravo, A. P. Sewell, J. Cummins, L. Flamand, J. M. Juteau, D. I. Bernstein and A. Vaillant, *Viol. J.*, 2009, **6**, 214.
- 165 D. I. Bernstein, N. Goyette, R. Cardin, E. R. Kern, G. Boivin, J. Ireland, J. M. Juteau and A. Vaillant, *Antimicrob. Agents Chemother.*, 2008, **52**, 2727–2733.
- 166 M. Blanchet, V. Sinnathamby, A. Vaillant and P. Labonté, *Antiviral Res.*, 2019, **164**, 97–105.
- 167 M. L. Guzmán, R. H. Manzo and M. E. Olivera, *Mol. Pharm.*, 2012, **9**, 2424–2433.
- 168 R. V. Alasino, I. D. Bianco, M. S. Vitali, J. A. Zarzur and D. M. Beltramo, *Macromol. Biosci.*, 2007, **7**, 1132–1138.
- 169 Y. Wang, T. D. Canady, Z. Zhou, Y. Tang, D. N. Price, D. G. Bear, E. Y. Chi, K. S. Schanze and D. G. Whitten, *ACS Appl. Mater. Interfaces*, 2011, **3**, 2209–2214.
- 170 T. D. Martin, E. H. Hill, D. G. Whitten, E. Y. Chi and D. G. Evans, *Langmuir*, 2016, **32**, 12542–12551.
- 171 A. Kuroki, J. Tay, G. H. Lee and Y. Y. Yang, *Adv. Healthcare Mater.*, 2021, **10**, 2101113.
- 172 A. Abbaszadegan, Y. Ghahramani, A. Gholami, B. Hemmateenejad, S. Dorostkar, M. Nabavizadeh and H. Sharghi, *J. Nanomater.*, 2015, **2015**, 720654.
- 173 W. Schreurs and H. Rosenberg, *J. Bacteriol.*, 1982, **152**, 7–13.
- 174 M. Ansari, H. Khan, A. Khan, S. S. Cameotra, Q. Saquib and J. Musarrat, *J. Appl. Microbiol.*, 2014, **116**, 772–783.
- 175 A. R. Nalwade and A. Jadhav, *Arch. Appl. Sci. Res.*, 2013, **5**, 45–49.
- 176 I. Sondi and B. Salopek-Sondi, *J. Colloid Interface Sci.*, 2004, **275**, 177–182.
- 177 S. Pal, Y. K. Tak and J. M. Song, *Appl. Environ. Microbiol.*, 2007, **73**, 1712–1720.
- 178 J. Yu, W. Zhang, Y. Li, G. Wang, L. Yang, J. Jin, Q. Chen and M. Huang, *Biomed. Mater.*, 2014, **10**, 015001.
- 179 A. Lesniak, A. Salvati, M. J. Santos-Martinez, M. W. Radomski, K. A. Dawson and C. Åberg, *J. Am. Chem. Soc.*, 2013, **135**, 1438–1444.
- 180 A. Kędziora, M. Speruda, E. Krzyżewska, J. Rybka, A. Łukowiak and G. Bugla-Płoskońska, *Int. J. Mol. Sci.*, 2018, **19**, 444.
- 181 C.-N. Lok, C.-M. Ho, R. Chen, Q.-Y. He, W.-Y. Yu, H. Sun, P. K.-H. Tam, J.-F. Chiu and C.-M. Che, *J. Proteome Res.*, 2006, **5**, 916–924.
- 182 U. Klueh, V. Wagner, S. Kelly, A. Johnson and J. Bryers, *J. Biomed. Mater. Res.*, 2000, **53**, 621–631.
- 183 J. R. Morones, J. L. Elechiguerra, A. Camacho, K. Holt, J. B. Kouri, J. T. Ramírez and M. J. Yacaman, *Nanotechnology*, 2005, **16**, 2346.
- 184 Q. L. Feng, J. Wu, G. Q. Chen, F. Cui, T. Kim and J. Kim, *J. Biomed. Mater. Res.*, 2000, **52**, 662–668.
- 185 A. K. Chatterjee, R. Chakraborty and T. Basu, *Nanotechnology*, 2014, **25**, 135101.
- 186 R. Bhattacharya and P. Mukherjee, *Adv. Drug Delivery Rev.*, 2008, **60**, 1289–1306.
- 187 M. Radzig, V. Nadtochenko, O. Koksharova, J. Kiwi, V. Lipasova and I. Khmel, *Colloids Surf., B*, 2013, **102**, 300–306.
- 188 T. Parandhaman, A. Das, B. Ramalingam, D. Samanta, T. Sastry, A. B. Mandal and S. K. Das, *J. Hazard. Mater.*, 2015, **290**, 117–126.
- 189 W. K. Jung, H. C. Koo, K. W. Kim, S. Shin, S. H. Kim and Y. H. Park, *Appl. Environ. Microbiol.*, 2008, **74**, 2171–2178.
- 190 M. K. Rai, S. Deshmukh, A. Ingle and A. Gade, *J. Appl. Microbiol.*, 2012, **112**, 841–852.
- 191 Y. H. Leung, A. M. Ng, X. Xu, Z. Shen, L. A. Gethings, M. T. Wong, C. M. Chan, M. Y. Guo, Y. H. Ng and A. B. Djurišić, *Small*, 2014, **10**, 1171–1183.
- 192 Y. Li, W. Zhang, J. Niu and Y. Chen, *ACS Nano*, 2012, **6**, 5164–5173.



- 193 E. Cabisco, J. Tamarit and J. Ros, *Int. Microbiol.*, 2000, **3**(1), 3–8.
- 194 S. R. Sarker, M. Hossain, S. A. Polash, M. Takikawa, R. D. Shubhra, T. Saha, Z. Islam, M. Hossain, M. Hasan and S. Takeoka, *Front. Bioeng. Biotechnol.*, 2019, **7**, 239.
- 195 R. Dutta, B. P. Nenavathu, M. K. Gangishetty and A. Reddy, *Colloids Surf., B*, 2012, **94**, 143–150.
- 196 Y.-M. Zhang and C. O. Rock, *Nat. Rev. Microbiol.*, 2008, **6**, 222–233.
- 197 D. R. Janero, *Free Radicals Biol. Med.*, 1990, **9**, 515–540.
- 198 C. Gaucher, A. Boudier, J. Bonetti, I. Clarot, P. Leroy and M. Parent, *Antioxidants*, 2018, **7**, 62.
- 199 O. Choi and Z. Hu, *Environ. Sci. Technol.*, 2008, **42**, 4583–4588.
- 200 A. Kumar, A. K. Pandey, S. S. Singh, R. Shanker and A. Dhawan, *Free Radicals Biol. Med.*, 2011, **51**, 1872–1881.
- 201 R. J. Barnes, R. Molina, J. Xu, P. J. Dobson and I. P. Thompson, *J. Nanopart. Res.*, 2013, **15**, 1432.
- 202 X. Dong, W. Liang, M. J. Meziani, Y.-P. Sun and L. Yang, *Theranostics*, 2020, **10**, 671.
- 203 J. Deutscher and M. H. Saier Jr., *J. Mol. Microbiol. Biotechnol.*, 2005, **9**, 125–131.
- 204 S. Shrivastava, T. Bera, A. Roy, G. Singh, P. Ramachandrarao and D. Dash, *Nanotechnology*, 2007, **18**, 225103.
- 205 B. Sohm, F. Immel, P. Bauda and C. Pagnout, *Proteomics*, 2015, **15**, 98–113.
- 206 N. Gou, A. Onnis-Hayden and A. Z. Gu, *Environ. Sci. Technol.*, 2010, **44**, 5964–5970.
- 207 D. A. Pelletier, A. K. Suresh, G. A. Holton, C. K. McKeown, W. Wang, B. Gu, N. P. Mortensen, D. P. Allison, D. C. Joy and M. R. Allison, *Appl. Environ. Microbiol.*, 2010, **76**, 7981–7989.
- 208 H. H. Lara, N. V. Ayala-Nuñez, L. Ixtepan-Turrent and C. Rodriguez-Padilla, *J. Nanobiotechnol.*, 2010, **8**, 1–10.
- 209 X. Hang, H. Peng, H. Song, Z. Qi, X. Miao and W. Xu, *J. Virol. Methods*, 2015, **222**, 150–157.
- 210 X. Dong, M. M. Moyer, F. Yang, Y.-P. Sun and L. Yang, *Sci. Rep.*, 2017, **7**, 1–10.
- 211 S. Huang, J. Gu, J. Ye, B. Fang, S. Wan, C. Wang, U. Ashraf, Q. Li, X. Wang and L. Shao, *J. Colloid Interface Sci.*, 2019, **542**, 198–206.
- 212 Z. Ramezani, M. R. Dayer, S. Noorizadeh and M. Thompson, *COVID*, 2021, **1**, 120–129.
- 213 Y. Abo-Zeid, N. S. Ismail, G. R. McLean and N. M. Hamdy, *Eur. J. Pharm. Sci.*, 2020, **153**, 105465.
- 214 P. Merkl, S. Long, G. M. McInerney and G. A. Sotiriou, *Nanomaterials*, 2021, **11**, 1312.
- 215 N. Mazurkova, Y. E. Spitsyna, N. Shikina, Z. Ismagilov, S. Zagrebel'nyi and E. Ryabchikova, *Nanotechnol. Russ.*, 2010, **5**, 417–420.
- 216 H. Ghaffari, A. Tavakoli, A. Moradi, A. Tabarraei, F. Bokharaei-Salim, M. Zahmatkeshan, M. Farahmand, D. Javanmard, S. J. Kiani and M. Esghaei, *J. Biomed. Sci.*, 2019, **26**, 1–10.
- 217 A. Tavakoli, A. Ataei-Pirkooh, G. M. Sadeghi, F. Bokharaei-Salim, P. Sahrapour, S. J. Kiani, M. Moghoofei, M. Farahmand, D. Javanmard and S. H. Monavari, *Nanomedicine*, 2018, **13**, 2675–2690.
- 218 T. Du, J. Liang, N. Dong, J. Lu, Y. Fu, L. Fang, S. Xiao and H. Han, *ACS Appl. Mater. Interfaces*, 2018, **10**, 4369–4378.
- 219 T. Du, J. Liang, N. Dong, L. Liu, L. Fang, S. Xiao and H. Han, *Carbon*, 2016, **110**, 278–285.
- 220 S. Gurunathan, M. Qasim, Y. Choi, J. T. Do, C. Park, K. Hong, J.-H. Kim and H. Song, *Nanomaterials*, 2020, **10**, 1645.
- 221 S. Kang, M. Pinault, L. D. Pfefferle and M. Elimelech, *Langmuir*, 2007, **23**, 8670–8673.
- 222 D. P. Linklater, M. De Volder, V. A. Baulin, M. Werner, S. JESSL, M. Golozar, L. Maggini, S. Rubanov, E. Hanssen and S. Juodkazis, *ACS Nano*, 2018, **12**, 6657–6667.
- 223 C. Yang, J. Mamouni, Y. Tang and L. Yang, *Langmuir*, 2010, **26**, 16013–16019.
- 224 H. Chen, B. Wang, D. Gao, M. Guan, L. Zheng, H. Ouyang, Z. Chai, Y. Zhao and W. Feng, *Small*, 2013, **9**, 2735–2746.
- 225 K. Rajavel, R. Gomathi, S. Manian and R. T. Rajendra Kumar, *Langmuir*, 2014, **30**, 592–601.
- 226 C. D. Vecitis, K. R. Zodrow, S. Kang and M. Elimelech, *ACS Nano*, 2010, **4**, 5471–5479.
- 227 S. Kang, M. Herzberg, D. F. Rodrigues and M. Elimelech, *Langmuir*, 2008, **24**, 6409–6413.
- 228 H. Chen, S. T. Humes, S. E. Robinson, J. C. Loeb, I. V. Sabaraya, N. B. Saleh, R. B. Khattri, M. E. Merritt, C. J. Martyniuk and J. A. Lednicky, *Nanotoxicology*, 2019, **13**, 1176–1196.
- 229 P. Sanpui, X. Zheng, J. C. Loeb, J. H. Bisesi Jr., I. A. Khan, A. N. Afrooz, K. Liu, A. R. Badireddy, M. R. Wiesner and P. L. Ferguson, *Part. Fibre Toxicol.*, 2014, **11**, 66.
- 230 X. Zou, L. Zhang, Z. Wang and Y. Luo, *J. Am. Chem. Soc.*, 2016, **138**, 2064–2077.
- 231 F. Perreault, A. F. De Faria, S. Nejati and M. Elimelech, *ACS Nano*, 2015, **9**, 7226–7236.
- 232 I. Zucker, J. R. Werber, Z. S. Fishman, S. M. Hashmi, U. R. Gabinet, X. Lu, C. O. Osuji, L. D. Pfefferle and M. Elimelech, *Environ. Sci. Technol. Lett.*, 2017, **4**, 404–409.
- 233 X. Lu, X. Feng, J. R. Werber, C. Chu, I. Zucker, J.-H. Kim, C. O. Osuji and M. Elimelech, *Proc. Natl. Acad. Sci. U. S. A.*, 2017, **114**, E9793–E9801.
- 234 R. Wu, X. Ou, R. Tian, J. Zhang, H. Jin, M. Dong, J. Li and L. Liu, *Nanoscale*, 2018, **10**, 20162–20170.
- 235 S. Liu, M. Hu, T. H. Zeng, R. Wu, R. Jiang, J. Wei, L. Wang, J. Kong and Y. Chen, *Langmuir*, 2012, **28**, 12364–12372.
- 236 O. Akhavan, E. Ghaderi and A. Esfandiari, *J. Phys. Chem. B*, 2011, **115**, 6279–6288.
- 237 J. Chen, H. Peng, X. Wang, F. Shao, Z. Yuan and H. Han, *Nanoscale*, 2014, **6**, 1879–1889.
- 238 M. Dallavalle, M. Calvaresi, A. Bottoni, M. Melle-Franco and F. Zerbetto, *ACS Appl. Mater. Interfaces*, 2015, **7**, 4406–4414.
- 239 V. T. Pham, V. K. Truong, M. D. Quinn, S. M. Notley, Y. Guo, V. A. Baulin, M. Al Kobaisi, R. J. Crawford and E. P. Ivanova, *ACS Nano*, 2015, **9**, 8458–8467.

- 240 Y. Tu, M. Lv, P. Xiu, T. Huynh, M. Zhang, M. Castelli, Z. Liu, Q. Huang, C. Fan and H. Fang, *Nat. Nanotechnol.*, 2013, **8**, 594.
- 241 S. Liu, T. H. Zeng, M. Hofmann, E. Burcombe, J. Wei, R. Jiang, J. Kong and Y. Chen, *ACS Nano*, 2011, **5**, 6971–6980.
- 242 X. Yang, J. Li, T. Liang, C. Ma, Y. Zhang, H. Chen, N. Hanagata, H. Su and M. Xu, *Nanoscale*, 2014, **6**, 10126–10133.
- 243 T. I. Kim, J. Kim, I.-J. Park, K.-O. Cho and S.-Y. Choi, *2D Mater.*, 2019, **6**, 025025.
- 244 S. Roy, A. Mondal, V. Yadav, A. Sarkar, R. Banerjee, P. Sanpui and A. Jaiswal, *ACS Appl. Bio Mater.*, 2019, **2**, 2738–2755.
- 245 X. Liu, G. Duan, W. Li, Z. Zhou and R. Zhou, *RSC Adv.*, 2017, **7**, 37873–37880.
- 246 G. R. Navale, C. S. Rout, K. N. Gohil, M. S. Dharne, D. J. Late and S. S. Shinde, *RSC Adv.*, 2015, **5**, 74726–74733.
- 247 A. Arabi Shamsabadi, M. Sharifian Gh, B. Anasori and M. Soroush, *ACS Sustainable Chem. Eng.*, 2018, **6**, 16586–16596.
- 248 Z. Xiong, X. Zhang, S. Zhang, L. Lei, W. Ma, D. Li, W. Wang, Q. Zhao and B. Xing, *Ecotoxicol. Environ. Saf.*, 2018, **161**, 507–514.
- 249 X. Liu, S. Sen, J. Liu, I. Kulaots, D. Geohegan, A. Kane, A. A. Puzos, C. M. Rouleau, K. L. More and G. T. R. Palmore, *Small*, 2011, **7**, 2775–2785.
- 250 S. Gurunathan, J. W. Han, A. A. Dayem, V. Eppakayala and J.-H. Kim, *Int. J. Nanomed.*, 2012, **7**, 5901.
- 251 S. Gurunathan, J. W. Han, A. A. Dayem, V. Eppakayala, M.-R. Park, D.-N. Kwon and J.-H. Kim, *J. Ind. Eng. Chem.*, 2013, **19**, 1280–1288.
- 252 J. Chen, X. Wang and H. Han, *J. Nanopart. Res.*, 2013, **15**, 1658.
- 253 Y. L. F. Musico, C. M. Santos, M. L. P. Dalida and D. F. Rodrigues, *ACS Sustainable Chem. Eng.*, 2014, **2**, 1559–1565.
- 254 J. D. West and L. J. Marnett, *Chem. Res. Toxicol.*, 2006, **19**, 173–194.
- 255 K. Krishnamoorthy, M. Veerapandian, L.-H. Zhang, K. Yun and S. J. Kim, *J. Phys. Chem. C*, 2012, **116**, 17280–17287.
- 256 P. Kumar, S. Roy, A. Sarkar and A. Jaiswal, *ACS Appl. Mater. Interfaces*, 2021, **13**, 12912–12927.
- 257 J. Li, G. Wang, H. Zhu, M. Zhang, X. Zheng, Z. Di, X. Liu and X. Wang, *Sci. Rep.*, 2014, **4**, 1–8.
- 258 S. Ye, K. Shao, Z. Li, N. Guo, Y. Zuo, Q. Li, Z. Lu, L. Chen, Q. He and H. Han, *ACS Appl. Mater. Interfaces*, 2015, **7**, 21571–21579.
- 259 M. Sametband, I. Kalt, A. Gedanken and R. Sarid, *ACS Appl. Mater. Interfaces*, 2014, **6**, 1228–1235.
- 260 M. Singh, C. Zannella, L. Altucci, F. Bajardi, A. Chianese, A. Damasco, M. R. Del Sorbo, R. di Girolamo, V. Foliero and G. Franci, *Front. Bioeng. Biotechnol.*, 2020, **8**, 1056.
- 261 Z. Song, X. Wang, G. Zhu, Q. Nian, H. Zhou, D. Yang, C. Qin and R. Tang, *Small*, 2015, **11**, 1171–1176.
- 262 R. Pokhrel, N. Bhattarai, K. A. Johnson, B. S. Gerstman, R. V. Stahelin and P. P. Chapagain, *Biochem. Biophys. Res. Commun.*, 2017, **493**, 176–181.
- 263 B. Luan, T. Huynh, L. Zhao and R. Zhou, *ACS Nano*, 2015, **9**, 663–669.
- 264 M. A. Unal, F. Bayrakdar, H. Nazir, O. Besbinar, C. Gurcan, N. Lozano, L. M. Arellano, S. Yalcin, O. Panatli and D. Celik, *Small*, 2021, **17**, 2101483.
- 265 J. Wang, Y. Yu, T. Leng, Y. Li and S.-T. Lee, *ACS Appl. Mater. Interfaces*, 2021, **14**(1), 191–200.
- 266 M. Khedri, R. Maleki, M. Dahri, M. M. Sadeghi, S. Rezvantlab, H. A. Santos and M.-A. Shahbazi, *Drug Delivery Transl. Res.*, 2021, 1–15.
- 267 M. Fukuda, M. S. Islam, R. Shimizu, H. Nassar, N. N. Rabin, Y. Takahashi, Y. Sekine, L. F. Lindoy, T. Fukuda and T. Ikeda, *ACS Appl. Nano Mater.*, 2021, **4**, 11881–11887.
- 268 I. S. Donskyi, C. Nie, K. Ludwig, J. Trimpert, R. Ahmed, E. Quaas, K. Achazi, J. Radnik, M. Adeli and R. Haag, *Small*, 2021, **17**, 2007091.
- 269 F. De Maio, V. Palmieri, G. Babini, A. Augello, I. Palucci, G. Perini, A. Salustri, P. Spilman, M. De Spirito and M. Sanguinetti, *Iscience*, 2021, **24**, 102788.
- 270 Z. Lin, Z. Wang, X. Zhang and D. Diao, *Nano Res.*, 2021, **14**, 1110–1115.